Aus der Klinik für Augenheilkunde
der Medizinischen Fakultät Charité – Universitätsmedizin Berlin

DISSERTATION

Influence of L-carnitine on transient receptor potential vanilloid 1 (TRPV1) activity in human corneal keratocytes

zur Erlangung des akademischen Grades
Doctor medicinae (Dr. med.)

vorgelegt der Medizinischen Fakultät
Charité – Universitätsmedizin Berlin

von

Elizabeth Turan

aus Berlin

Datum der Promotion: 03.03.2023

Preface

Parts of this thesis have already been published in:

1. Turker E, Garreis F, Khajavi N, Reinach PS, Joshi P, Brockmann T, Lucius A, Ljubojevic N, Turan E, Cooper D, Schick F, Reinholz R, Pleyer U, Kohrle J, Mergler S. Vascular endothelial growth factor (VEGF) induced downstream responses to transient receptor potential vanilloid 1 (TRPV1) and 3-Iodothyronamine (3-T1AM) in human corneal keratocytes. Front Endocrinol (Lausanne). 2018;9:670.
2. Turan E, Valtink M, Reinach PS, Skupin A, Luo H, Brockmann T, Ba Salem MHO, Pleyer U, Mergler S. L-carnitine suppresses transient receptor potential vanilloid type 1 activity and myofibroblast transdifferentiation in human corneal keratocytes. Lab Invest. 2021;101(6):680-9.

Dedicated to

Neil and Sariye Turan

Table of Contents

Abbreviations

$3T_1AM$	3-Iodothyronamine
αSMA	alpha-smooth muscle actin
Ca^{2+}	calcium
$[Ca^{2+}]_i$	intracellular calcium concentration
CAP	capsaicin
CB	cannabinoid receptor
CD	cluster of differentiation
Cl^-	chloride
CPZ	capsazepine
DES/ DED	dry eye syndrome/ disease
DMEM	Dulbecco's Modified Eagle's Medium
DMSO	Dimethyl sulfoxide
EGFR	Epidermal growth factor receptor
f_{340nm}/f_{380nm}	fluorescence ratio between 340 and 380 nm
FCS	fetal calf serum
Fura-2/AM	fura-2/acetoxymethyl ester
HCEC	human corneal epithelial cells
HCEC-12	human corneal endothelial cells
HCF	human corneal fibroblasts
HCjEC	human conjunctival epithelial cells
HCK	human corneal keratocytes
HCLEC	human corneal limbal epithelial cells
HP	holding potential
hPtEC	immortalized pterygial epithelial cells

IL	interleukin
MAPK	mitogen-activated protein kinase
MGD	meibomian gland dysfunction/disease
MMP	matrix metalloproteinase
Na^+	sodium
NGF	nerve growth factor
NK	neurotrophic keratopathy
OCT	organic cation transporter
pA/pF	current density (current capacity pA/cell membrane capacity pF)
PBS	phosphate-buffered saline
PDGF	platelet-derived growth factor
ROI	region of interest
RPE	retinal pigment epithelium
Rs	series resistance
SEM	standard error of the mean
TGF	transforming growth factor
TNFα	tumor necrosis factor alpha
TRPs	transient receptor potential channels
TRPA	TRP ankyrin receptor
TRPC	TRP canonical receptor
TRPM	TRP melastatin receptor
TRPML	TRP mucolipin receptor
TRPN	TRP NO-mechanoreceptor (NOMP)
TRPP	TRP polycystin receptor
TRPV	TRP vanilloid receptor

Abstract

Background/Aims: Transient receptor potential vanilloid 1 (TRPV1) belongs to the vanilloid TRP channel family and was first known as a pain receptor which can be activated by capsaicin (CAP), the pungent ingredient in hot chili peppers. Since TRPV1 is expressed in corneal tissues including corneal nerve fibers, there is substantive evidence that functional TRPV1 expression has important roles in controlling corneal transparency, which is required for normal vision. On the one hand, this channel is involved in wound healing processes by promoting stromal fibroblast transdifferentiation into myofibroblasts. On the other hand, TRPV1 activation can lead to calcium influx and the release of proinflammatory cytokines triggering inflammatory ocular surface diseases. Due to these novel roles of TRPV1, its characterization in each corneal cell layer is essential to elucidate the promoting or inhibiting influence of endogenous modulators on this channel activity. This insight may help to identify novel procedures for improving therapeutic management of wound healing. Previous studies suggested that L-carnitine has osmoprotective effects in human corneal and conjunctival epithelial cells, elicited through the suppression of hypertonic-induced TRPV1 activation. In this thesis, the inhibitory influence of L-carnitine on TRPV1 activity in immortalized human corneal keratocytes (HCK) was investigated. **Methods:** The planar patch-clamp technique was used to record whole-cell currents of TRPV1 in an established HCK cell line. In addition, the intracellular calcium concentration ($[Ca^{2+}]_i$) was measured using fluorescence calcium imaging, whereby the fluorescence ratio (f_{340nm}/f_{380nm}) is proportional to $[Ca^{2+}]_i$. The effect of L-carnitine was investigated on heat-, hypertonic-, and CAP-induced TRPV1 activation. **Results:** 1 mM L-carnitine inhibited increases of $[Ca^{2+}]_i$ induced by either hypertonic stress (450 mOsM), temperature rise (≈ 43 °C) or extracellular application of 10 µM CAP. In parallel with the calcium regulation, L-carnitine also suppressed the underlying increases in ionic currents induced by TRPV1 activation. **Conclusion:** There is functional TRPV1 expression in HCK. Furthermore, an inhibiting effect of L-carnitine on TRPV1 activity was evidenced in HCK for the first time. In a clinical context, these findings suggest a protective effect of L-carnitine against TRPV1-induced $[Ca^{2+}]_i$ increases and hold promise for reducing stromal scarring through corneal wound healing.

Zusammenfassung

Hintergrund/Zielsetzung: Der Transient Rezeptor Potential Vanilloid 1 (TRPV1) ist der bekannteste Vertreter der TRP-Kanal Familie und kann durch Capsaicin aktiviert werden (Capsaicin-Rezeptor). *In vitro* Studien haben zeigen können, dass der TRPV1 nicht nur im peripheren und zentralen Nervensystem, sondern auch in nichtneuronalen Zellen der Augenoberfläche vorkommt. Durch seine Expression im Hornhautgewebe übernimmt er eine wichtige Rolle in der Aufrechterhaltung der Hornhauttransparenz, welche für einen klaren Seheindruck entscheidend ist. Einerseits ist der TRPV1 in Prozessen der stromalen Wundheilung involviert. Andererseits erhöht seine Aktivierung den Calciumeinstrom sowie die Freisetzung proinflammatorischer Zytokine, welche zu entzündlichen Reaktionen der Augenoberfläche führen. In Hinblick auf mögliche Therapieansätze ist eine nähere Charakterisierung dieser nicht-klassischen TRPV1 Funktion in den einzelnen Hornhautschichten des Auges entscheidend. Bisherige Studien haben zeigen können, dass L-Carnitin durch seinen hemmenden Einfluss auf den TRPV1 einen osmoprotektiven Effekt sowohl im Hornhaut- als auch Bindehautepithel aufweist. Die vorliegende Arbeit beschäftigt sich mit dem Effekt von L-Carnitin auf den TRPV1 induzierten Calciumanstieg in humanen Hornhautkeratozyten (HCK). **Methoden:** Eine etablierte SV40-transfizierte HCK Zelllinie wurde als HCK Modell verwendet. Mit der planaren Patch-Clamp-Technik wurden Ganzzellströme nach TRPV1 Aktivierung in Ab- und Anwesenheit von L-Carnitin gemessen. Ferner wurden Fluoreszenzsignale (f_{340nm}/f_{380nm}), welche proportional zur intrazellulären Calciumkonzentration sind, mittels Fluoreszenz Calcium Imaging Verfahren aufgezeichnet. Hierbei wurde der Einfluss von L-Carnitin auf den durch Hitze (≈ 43 °C), Hyperosmolarität (450 mOsM) und Capsaicin (10 µM) aktivierten TRPV1 untersucht. **Ergebnisse:** 1 mM L-Carnitin reduziert die intrazelluläre Calciumkonzentration in HCK Zellen durch Hemmung des TRPV1 Kanals. Zudem konnte gezeigt werden, dass L-Carnitin die durch Capsaicin erhöhten TRPV1 Ionenströme unterdrückt. **Schlussfolgerung:** Funktionale TRPV1 Expression liegt auch in stromalen HCK Zellen vor. Erstmalig konnte der hemmende Einfluss von L-Carnitin auf den TRPV1 Kanal in HCK Zellen nachgewiesen werden. Diese Ergebnisse deuten darauf hin, dass L-Carnitin einen protektiven Einfluss auf durch erhöhte TRPV1 Aktivität hervorgerufene Augenschäden haben könnte. L-Carnitin könnte somit einen vielversprechenden therapeutischen Ansatz sowohl in der Vorbeugung als auch Behandlung stromaler Hornhautverletzungen darstellen.

1. Introduction

1.1 Anatomy and function of the human cornea

The avascular transparent cornea layer is located at the outermost part of the ocular surface and has an horizontal diameter of about 11 mm (1) and a central thickness of around 560 µm (2). Nearly 90 % of the cornea consists of stroma, the middle connective tissue between the epithelium and endothelium, and it has a central thickness of 465 – 500 µm (2-4). The corneal epithelium, with a thickness of approximately 50 µm (2), is located at the outside facing the air, while the endothelium (4 - 6 µm thick) forms the undermost layer at the posterior cornea (5). In addition to these three cellular layers (epithelium, stroma, endothelium), the cornea also contains two interface basement membranes: the Bowman membrane (~ 16 µm thick) (2) located between the epithelium and stroma as well as the Descemet membrane (8 – 10 µm thick) located between the stroma and endothelium (6) (Fig.1). In 2013, an acellular membrane called Dua's layer (6 – 13 µm thick) was first detected between the stroma and Descemet membrane (7).

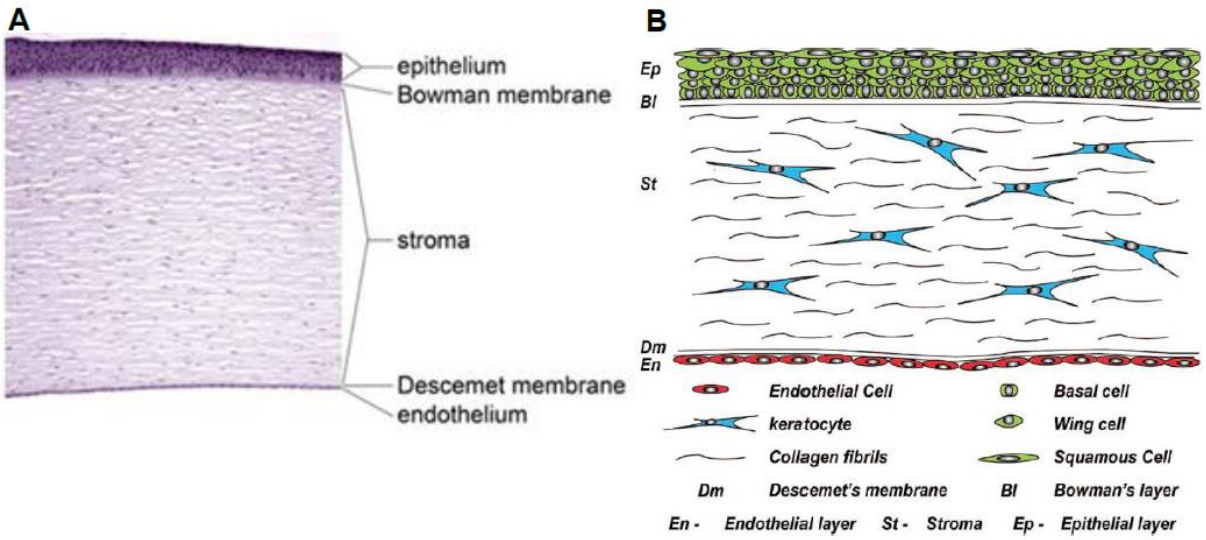

Figure 1: Vertical anatomy of the human cornea. A: Histological structure of the human eye cornea; magnification x100. The corneal epithelium is located above the Bowman membrane at the outmost part of the cornea, while the endothelium is located under the Descemet membrane at the posterior cornea. The corneal stroma is located between the epithelial and endothelial layers. [Image kindly provided by M. Valtink (8)]. **B:** Schematic structure of the cornea. The corneal stroma embraces most of the corneal tissue containing keratocytes (blue stained cells), from which are derived fibroblasts and myofibroblasts interspersed between collagen fibrils. [Secker et al. (9)].

The cornea as the window of the eye is involved in light refraction as well as protection against external stimuli and keeps the rigidity of the eyeball. Due to the fact that the cornea mainly contributes to light refraction, its transparency plus smooth and intact curvature are relevant for good vision.

The cornea is sensory innervated by the ophthalmic branch of the trigeminal nerve (10). The nerves enter the cornea in the middle third of the stroma, divide into smaller branches forming the subepithelial nerve plexus as well as the subbasal epithelial nerve plexus and innervate the cornea from the epithelial cell layer to the mid stroma (11-15) (Fig. 2).

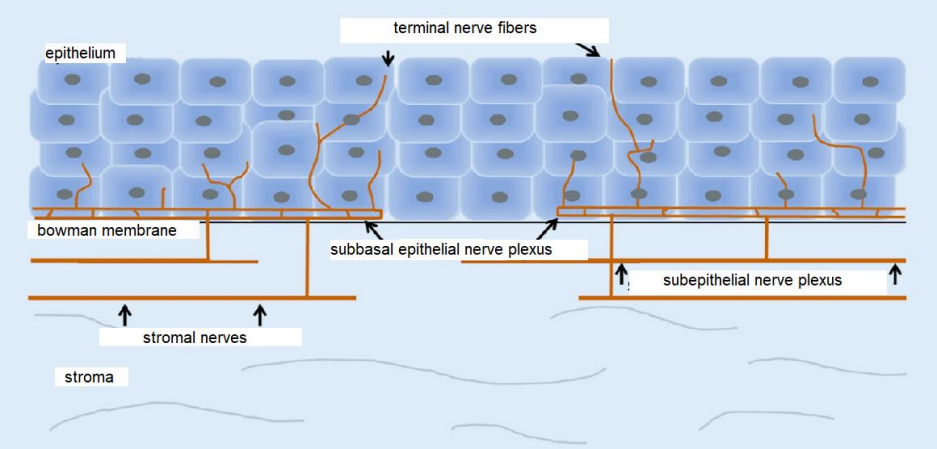

Figure 2: Schematic image of corneal innervation. From the limbal plexus, corneal nerves enter the mid stroma and run forward anteriorly toward the central area (reviewed in (15)). Between the Bowman layer and the anterior stroma, the stromal nerves form the subepithelial nerve plexus (reviewed in (15)). Then, they perforate the Bowman layer forming the subbasal epithelial nerve plexus and terminate within the superficial epithelial layer (reviewed in (15)). [Image modified after Mertsch et al. (16)].

The cornea not only consists of the aforementioned nonexcitable cells, but also contains excitable cells (nociceptors) in nerve fibers containing 7000 pain receptors per mm^2 reflecting the highest pain receptor density of the human body (10). Accordingly, the cornea has the highest sensitivity compared with other tissues in the entire body and is provided with oxygen and other important nutrients through aqueous humor, a vascular loop system, and the tear film (17). The cornea also participates in mediating dynamic processes including cell-cell and cell-extracellular matrix interactions, which are necessary for the maintenance of the corneal structure and function (17). A disturbance of this dynamic network-system may affect all corneal layers and may elicit inflammatory cytokines, leading to corneal destruction (17).

Furthermore, keratocytes located in the stroma have a crucial role regarding inflammatory processes and corneal wound healing and will be introduced in the next paragraph.

1.2 Human corneal keratocytes and ocular surface

The corneal stroma embraces most of the corneal tissue and contains water, keratocytes, proteoglycans, and collagen fibrils especially type I, III and V (18). Human corneal keratocytes (HCK) are mesenchymal-derived specialized fibroblasts in the stroma and are a population of normally quiescent cells (19, 20). The highest density of keratocytes is in the anterior 10 % of the stroma with ~ 20.500 cells/mm^3 (2). Since keratocytes produce collagen and proteoglycans, they contribute in maintaining corneal structure (21). Furthermore, HCK cells contain proteins such as so called crystallins in their cytoplasma, which maintain the transparency of the cornea (22). Since corneal keratocytes have a similar refractive index as the surrounding stroma, they are usually unseen (22). During activation, the relative proportion of these crystallin proteins diminishes, making the keratocytes visible (22). Their ability to proliferate and produce matrix metalloproteinases (MMP) shows their major role in healing processes and expressing inflammation signals (23). Functional interleukin (IL)-4 and IL-17-receptors are expressed on the surface of cultured HCK cells, suggesting that these cells may be involved in the control of corneal inflammation, since IL-4 and IL-17 are proinflammatory mediators (24, 25). Furthermore, HCK cells express clusters of differentiation (CD) 34 antigens on their surface, which enable leukocyte adhesion during inflammatory processes (26). The superficial epithelial layer of the cornea stabilizes the tear film, which is secreted for maintaining ocular surface health (27). It protects the eye against dehydration and guarantees the transparency needed for visual detection (27). Due to the avascular nature of the corneal stroma, keratocytes are dependent on the overlying epithelium (23, 28). In various studies, corneal epithelial-keratocyte cell interactions have been analyzed extensively (23, 29-36). In event of corneal injury, keratocytes are stimulated to either undergo apoptosis or to lose their quiescence and transmute into repair phenotypes (29-36). Firstly, cytokines such as tumor necrosis factor alpha (TNFα) and IL-1 are released from the overlying epithelium into the stroma resulting in apoptosis of the anterior stromal keratocytes (23, 29, 31, 34, 36). This initial HCK cell death functions to protect the

cornea from further inflammation and subsequent loss of visual transparency (23, 30). After apoptosis and mitosis, the migration of keratocytes from deeper stromal layers is induced by platelet-derived growth factor (PDGF), which replenishes the anterior stroma during wound healing (37). Additionally, in the event of basement membrane disruption, the corneal epithelium also secretes transforming growth factor (TGF)-β2, which can activate HCK and induce myofibroblastic transformation, leading to new extracellular matrix production (33, 35). These findings illustrate the major involvement of HCK in mediating inflammatory processes during corneal repair.

1.3 Transient receptor potential channels

Corneal keratocytes, like other cells, are regulated by calcium (Ca^{2+}) dependent cellular mechanisms. Transient receptor potential channels (TRPs) are substantially involved in Ca^{2+} regulation. TRPs were first detected in the fruit fly Drosophila (38) and include a large number of non-selective cation channels, which are mostly Ca^{2+} permeable (reviewed in (39)). Based on structure, stimulation, and phylogeny, there are 28 TRP subtypes, which are classified into the following 7 subfamilies: TRPC (canonical), TRPV (vanilloid), TRPM (melastatin), TRPN (no mechanoreceptor potential - NOMP), TRPA (ankyrin), TRPML (mucolipin), and TRPP (polycystin) (reviewed in (40)) (Fig. 3).

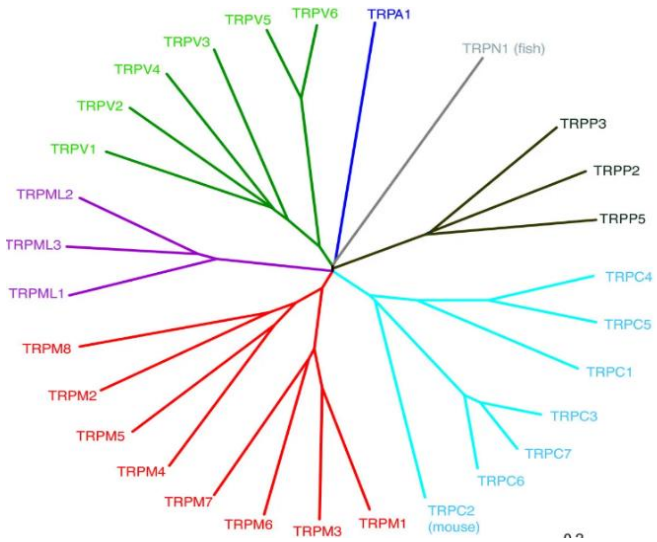

Figure 3: Phylogenetic tree of the mammalian TRP channel superfamily. Each TRP channel superfamily is marked with a different color. To date, TRPN has only been detected in worm, Drosophila, and zebrafish. [Nilius et al. (41)].

TRPs consist of six transmembrane helices (S1-S6), while segments S5 and S6 form a loop for the passage of cations (42). All TRPs, except TRPM4 and TRPM5, are Ca^{2+} permeable (43, 44). As polymodal channels, TRPs are activated by a host of stimuli such as temperature, osmotic or pH changes, mechanical stress or intracellular and extracellular ligands that mediate sensory transduction. Furthermore, they are involved in thermo- and osmosensation as well as in perceiving the five senses (vision, taste, olfaction, hearing and touch) (reviewed in (45)). In excitable cells, activation of TRPs increases the intracellular sodium (Na^+) and intracellular calcium concentration ($[Ca^{2+}]_i$), which leads to a depolarization of the cell membrane that in turn activates action potentials above a certain membrane voltage threshold (reviewed in (46)). An excessive Ca^{2+} influx may be a relevant modulator in the pathogenesis of ocular surface dystrophy, since numerous studies have demonstrated that dysfunction of voltage dependent ion channels and TRPs is related to increased cytosolic Ca^{2+} and apoptosis (47-49). TRPs are expressed in both excitable cells (neurons) and nonexcitable cells (50, 51). However, their functions - especially in nonexcitable cells - are not fully elucidated so far. Studies by Mergler and Reinach et al. show that TRPs are also expressed in corneal and conjunctival cell layers (8, 52-54) (Fig. 4).

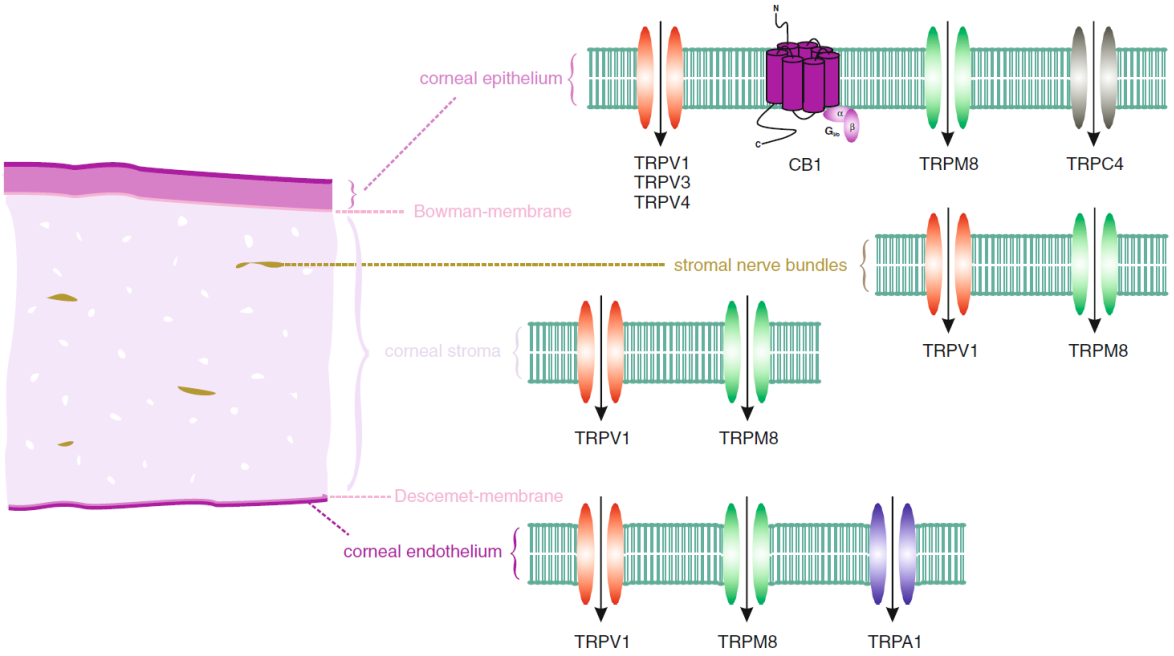

Figure 4: Localization of TRP channel expression in human corneal cell type layers. Corneal epithelium: TRPV1/3/4, cannabinoid receptor 1 (CB1), TRPC4, TRPM8; corneal stroma: TRPV1, TRPM8; corneal nerve fibers: TRPV1, TRPM8; corneal endothelium: TRPV1, TRPM8, TRPA1. [Image kindly provided by S. Mergler (52)].

1.4 Characterization of TRPV1

TRPV1, also known as capsaicin (CAP)-receptor, is a subtype of the aforementioned TRP family. Classically, TRPV1 as a pain receptor is mainly expressed in the peripheral or central nervous system (55-60) including afferent corneal nerve fibers (61, 62). Therefore, TRPV1 is responsible for the perception of temperature (heat from above 43 °C) as well as pain (especially from heat and spiciness) (55, 57, 63). Pharmacologically, TRPV1 can be selectively activated by CAP (55), the main pungent ingredient in hot chili peppers or by neurotoxin such as vanillotoxins (VaTxs), which occur in the venom of the tarantula “Psalmopoeus cambridgei” (64). Furthermore, TRPV1 can also be activated by pH reduction < 5.9 (63) as well as hyperosmotic challenge (65-69).

Investigations by Belmonte et al. (70), Mergler (54), and Reinach (67) revealed that the TRPV1 channel plays a central role in the pathogenesis of dry eye syndrome (DES)/ dry eye disease (DED). DES is an ocular surface disease connected with loss of homeostasis of the tear film and is one of the most common disorders in ophthalmological practice around the world. Its prevalence in the world population ranges between 6 – 34 %, with increasing tendency (71). In Central Europe, nearly 10 – 20 % of the population suffer from this disease (72). Women are more susceptible than men and the prevalence is age related (73, 74). Typical symptoms are redness, irritation, burning, and foreign body sensation. For the development of DES three main factors are involved, which affect each other and constitute a so called *circulus vitiosus* (Fig. 5).

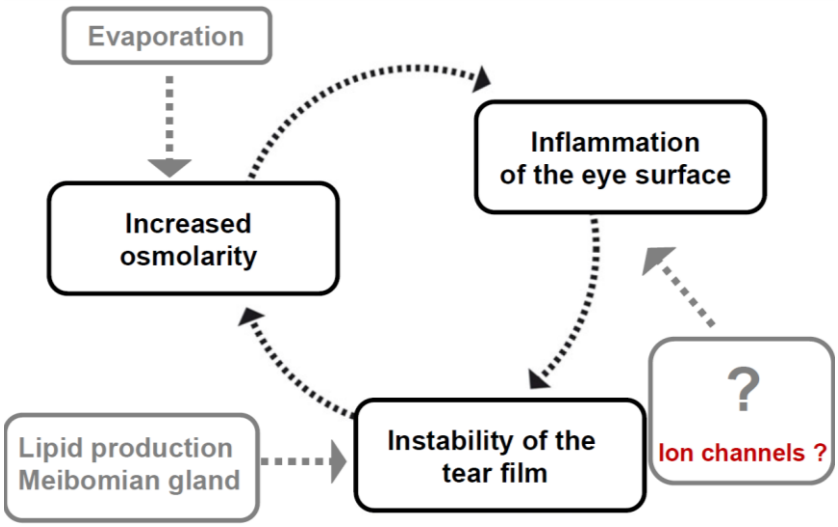

Figure 5: Schematic of the *circulus vitiosus*. Pathogenesis of DES with the three main factors and their triggers. [Image modified by S. Mergler (75)].

An unstable tear film caused by meibomian gland dysfunction (MGD) triggers DES (72). Specifically, the MGD includes a disturbed formation and secretion of lipids by the meibocytes, which are located in the eyelids. Notably, these lipids are essential for stabilizing the tear film and protect it against pathogenic germs. Due to inappropriate evaporation or aqueous deficiency (76) as well as impairment in corneal nerve innervation (77), the tear production becomes reduced, leading to a hypertonic tear film (78). The osmolarity of a healthy cornea is about 300 mOsM, whereas tear hyperosmolarity is defined by a referent of 316 mOsM (79). Regarding DES, TRPV1 activation by hyperosmolarity is a crucial point in connection with Ca^{2+} regulation, which unleashes an intracellular signaling cascade resulting in the release of pro-inflammatory cytokines such as IL-6 and IL-8 (67, 80). Furthermore, TRPV1 activation elicits epidermal growth factor receptor (EGFR) signaling transduction pathways, which in turn stimulate the activation of upstream mitogen-activated protein kinases (MAPK) linked with inflammatory processes (67, 81). Previous studies also revealed that injury-induced TRPV1 signaling is linked with TGF-β1-mediated transdifferentiation of HCK cells into myofibroblasts, leading to corneal fibrosis and opacification (82, 83).

1.5 L-carnitine

Carnitine, as a quaternary amino acid, occurs naturally in mammalian tissue with relatively high concentrations in heart and skeletal muscle (84). Mammals are able to generate carnitine by in situ biosynthesis using the amino acids methionine and lysine (85-87) (Fig.6).

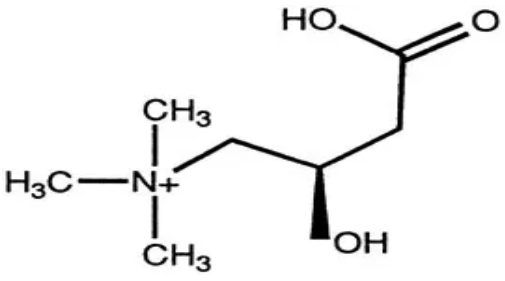

Figure 6: Chemical structure of L-carnitine. Carnitine is a water-soluble molecule and contains seven carbon atoms. Its chemical structure is 3-hydroxy-4-N-trimethylaminobutyric acid. The molecule exists in two stereochemical isomers - an active (L-carnitine) and an inactive form (D-carnitine). [Pettegrew et al. (88)].

It is involved in regulating the energy metabolism that is most known for mitochondrial oxidation of long chain fatty acids for energy production (89, 90). Therefore, carnitine enables the transport of these fatty acids into the mitochondria (91-93). Additionally, it converts the glucose metabolism from glycolysis to glycogen storage, leading to improvement of total glucose metabolism by increasing nonoxidative glucose disposal (94, 95).

L-carnitine is transported into human corneal limbal epithelial cells (HCLEC) and human conjunctival epithelial cells (HCjEC) by the carnitine/ organic cation transporter (OCT), which is Na^+-, energy-, time-, and pH-dependent (96). Under hyperosmotic stress these transporters are upregulated (96). Moreover, Pescosolido et al. detected lower carnitine levels in the tear film of dry eye patients and suggested that an imbalance in the concentration of carnitine molecules may partly be responsible for ocular cell damage from exposure to a hypertonic tear film (97). In this connection, further studies have demonstrated that L-carnitine has an osmoregulatory function as an osmoprotective agent against hyperosmotic stress, not only in human corneal epithelial cells (HCEC) but also in HCjEC (69, 98-101). The usage of eyedrops containing L-carnitine improves the common symptoms of dry eyes and also reduces the associated conjunctival staining (101). Due to hyperosmolarity-associated activation of TRPV1, Khajavi et al. demonstrated the reduction of hypertonic-induced shrinkage of HCjEC through an interaction of L-carnitine with TRPV1 channels (69). Furthermore, L-carnitine has also been shown to be capable of protecting human retinal pigment epithelium (RPE) cells from H_2O_2-induced oxidative damage (102). As a natural antioxidant, L-carnitine has shown potential to reduce stromal fibrosis (103). Since TRPV1 is involved in corneal opacification, the influence of L-carnitine on the TRPV1 activation in HCK is highlighted in this thesis.

1.6 Aims of research

The role of TRPV1 in connection with L-carnitine has recently been highlighted in ocular surface cells including conjunctiva cells, but not in HCK so far. Based on previous findings and the aforementioned phenomenon, this experimental study was focused on HCK and was undertaken to:

1. Characterize putative functional TRPV1 expression using three specific types of activation mechanisms:
    a) Physically by heat > 43 °C
    b) Osmotically using hypertonic solution (450 mOsM)
    c) Pharmacologically with 10 µM CAP
2. Investigate the effect of 1 mM L-carnitine on TRPV1-induced Ca^{2+} influx in HCK.
3. Investigate the effect of 1 mM L-carnitine on TRPV1-induced increases in whole-cell currents in HCK.

2. Materials and methods

2.1 Cell cultivation and preparation

Established SV40-transfected HCK cells were kindly provided by Zorn-Kruppa and colleagues from the University Medical Center Hamburg-Eppendorf (Hamburg, Germany) (104, 105). Generally, the cells were cultivated in an incubator at 37 °C, 95 % humidity and 5 % CO_2, and were cultivated in T25 flasks. 1 – 3 days before measurement, the cells had a final confluence of 60 – 80 %. For the cell passage, the cells were washed two times with 10 ml calcium- and magnesium-free phosphate-buffered saline (PBS). 1 ml accutase was used for detaching the cells from the flask surface. After approximately 5 minutes of incubation, the integrity of the dissociated cells (80 – 90 %) was confirmed by examining them under a light microscope. The enzymatic reaction was stopped by adding 10 ml medium containing fetal calf serum (FCS). To get a single cell suspension, the cells were pipetted gently up and down a few times. After that, the suspension was centrifuged (800 U/min, 100 g) preferably in a 15 ml tube for 5 minutes. Then, the supernatant was removed and the cells were resuspended in Dulbecco's Modified Eagle's Medium (DMEM) containing 10 % FCS and antibiotics (penicillin and streptomycin).

2.2 Chemicals and solutions

Supplements for cell culture and medium containing serum were purchased from Biochrom AG (Berlin, Germany) or Life Technologies Invitrogen (Karlsruhe, Germany). Accutase came from PAA Laboratories (Pasching, Austria) and fura-2/ acetoxymethyl ester (fura-2/AM) from TOCRIS Bioscience (Bristol, UK). CAP was purchased from the Cayman Chemical Company (Ann Arbor, Michigan, USA), while all other reagents were received from Sigma-Aldrich (Deisenhofen, Germany).

Name of chemicals	Stock concentration	Desired concentration	Desired Volume	Required volume
Fura-2/AM	1 mM (DMSO)	1 µM	1 ml	1 µl
CAP	100 mM (DMSO)	10 µM	10 ml	1 µl
L-carnitine	100 mM (water)	1 mM	1 ml	10 µl

Figure 7: Table of chemicals with their used concentration and volume.

2.3 Optical fluorescence measurements

2.3.1 Fluorescent dye fura-2/AM

Fura-2/AM is a membrane permeable derivative, which was developed to allow for an estimation of $[Ca^{2+}]_i$ (106). Fura-2/AM, with specific photometric properties, has two excitation wavelengths (340 and 380 nm) and one emission wavelength (510 nm) (106). While Ca^{2+}-saturated fura-2 is detected by 340 nm, Ca^{2+}-free fura-2 can be detected by 380 nm (106). Both fluorescence response signals are alternately measured through alternation of the excitation between the wavelengths of 340 and 380 nm (106). The fluorescence ratio (f_{340nm}/f_{380nm}) of these two fluorescence response signals can be calculated, which correlates proportionally with changes in $[Ca^{2+}]_i$ (106).

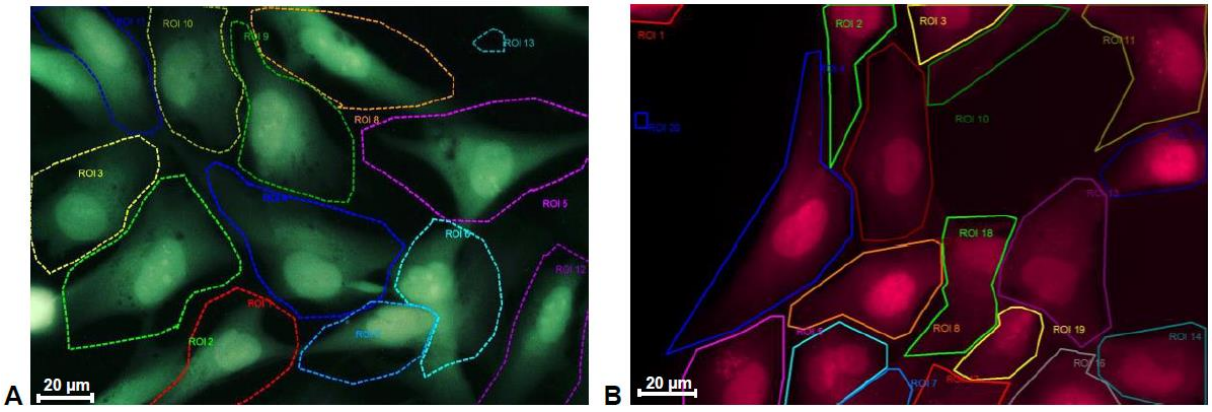

Figure 8: Fluorescence microscope image of fura-2/AM-loaded HCK cells. A: Fura-2/AM-loaded HCK cells detected by 340 nm wavelengths (green stained by the software). **B:** Fura-2/AM-loaded HCK cells detected by 380 nm wavelengths (red stained by the software). The emission wavelength was at 510 nm and was detected by a black and white camera (Olympus XM-10). The region of interest (ROI) was selected for single cell analysis (cellSense Olympus Software, Hamburg, Germany). [Images by E. Turan].

2.3.2 Fluorescence single cell calcium imaging

Cells are dependent on the regulation of their intracellular Ca^{2+} levels for the controlling of most of their important functions, from their origin at fertilization including muscle contraction, neuronal transmission, cellular motility and growth until their demise in apoptotic processes (107-110). Ca^{2+}, as an ubiquitous second messenger, plays a wide-ranging role in biological signaling pathways. It can affect the permeability and

activate ion channels, resulting in signaling transduction or acting directly on other effector proteins. In 1985, Roger Tsien and colleagues first established a highly sensitive functional assay called fluorescence calcium imaging to investigate the fluorescence-optic properties of cells, tissue or medium (106). This technique is used to measure very small changes in $[Ca^{2+}]_i$. In this study, fluorescence calcium imaging was used to monitor time dependent changes in cytosolic free $[Ca^{2+}]_i$ by measuring changes in fura-2/AM fluorescence intensity in HCK cells. For this purpose, the cells were cultivated on glass coverslips (15 mm diameter) and were placed in a culture plate until they reached a semi confluent stage (≈ 60 – 80 %) (111). HCK cells were preincubated with 1 µM fura-2/AM at 37 °C for 20 – 40 minutes and loading was stopped with a Ringer-like (control) solution containing (in mM): 150 NaCl, 6 CsCl, 1.5 $CaCl_2$, 1 $MgCl_2$, 10 HEPES-acid, and 10 glucose with pH 7.4 (osmolarity ≈ 300 mOsM) (111, 112). Instead of potassium, cesium was used to suppress potassium conductance (111). For the experiments using hypertonic challenge, 130 mM D-mannitol (osmolarity ≈ 450 mOsM) was added (69). The coverslips were placed in a bath chamber containing the same solution on an inverted microscope stage (Olympus BW50WI, Hamburg, Germany) connected to a digital imaging system (Olympus, Hamburg, Germany) (111).

Figure 9: Setup of the fluorescence calcium imaging. Located at the Charité University of Medicine – Campus Virchow Clinic, Department of Ophthalmology, Berlin, Germany. (1) Digital Olympus XM-10 camera, (2) coverslips on inverted microscope stage, (3) micromanipulator, (4) LED-Hub light source, (5) Omicron controller, (6) computer with digital imaging software system. [Images by E. Turan].

The calcium homeostasis (control baseline) should remain constant for 10 minutes and was routinely checked before each experiment (111). Depending on the experimental design, the measurements lasted between 5 and 10 minutes. The Life Science fluorescence cell imaging software “cellSens” (Olympus, Hamburg, Germany), along with a digital camera (Olympus XM-10), were used to alternatively gather and evaluate fura-2-induced fluorescence signals (111). Fura-2/AM fluorescence was alternately excited at 340 nm and 380 nm excitation wavelength and the emission was detected at 510 nm wavelength every 500 ms (250 – 3800 ms exposure time) (106, 111). An LED light source and specific filters (LED-Hub and software by Omicron, Rodgau-Dudenhoven, Germany) were used for the fluorescence excitation wavelengths (111). When a blocker was tested, cells were preincubated with the blocker for ~ 30 minutes and all measuring solutions contained the blocker (111). The TIDA software by HEKA electronics (Lamprecht, Germany) was used for evaluation (e.g., offsetting, drift corrections, normalization). The experiments were performed in a shaded, windowless room at a constant room temperature (≈ 22 °C). The results are shown as mean traces f_{340nm}/f_{380nm} ± standard error of the mean (SEM) (error bars in both directions), with n-values which indicate the number of experiments per data point. The fluorescence ratios were normalized (control set to 0.1) and averaged (with error bars).

2.4 Planar patch-clamp technique

In this thesis, a semi-automated planar patch-clamp setup was used (Port-a-Patch® Nanion), as described by Bruggemann et al. in 2006 (113). First of all, 5 µl of the internal solution (consisting of (in mM): 50 CsCl, 10 NaCl, 60 CsF, 20 EGTA, and 10 HEPES/ KOH (pH 7.2; osmolarity = 288 mOsmol)) was applied to the inside of the microchip (114). Then, the microchip was screwed onto a chip holder and the NanionControl software (Nanion Biotechnologies, Munich, Germany) was started. Thereafter, 5 µl of the cell suspension was additionally added to the drop of extracellular solution on the top of the chip. Subsequently, 5 µl cell suspension was added. An automated suction was applied by a software-controlled pump to move a single cell into the aperture of the microchip. The chip has a micro-opening of ≈ 1 – 3 µm, corresponding to a resistance of 3 – 5 MΩ to measure small ion channel currents. When a cell attached to the chip opening, additional suction pulses were needed for a cell-attached configuration and a seal enhancing solution was used shortly before. This

led to a significant increase of the seal resistance. Due to the fragile properties of HCK cells, breaking into the whole-cell configuration was easily achieved. PatchMaster software version 2.5 for Windows (HEKA, Lambrecht, Germany) in combination with an EPC10 amplifier were used for electrophysiological recordings, data acquisition, and evaluation. To eliminate any possible contributions by voltage dependent Ca^{2+} activity, the holding potential (HP) was set to 0 mV for the entire experiment. Additionally, a liquid junction potential of 4 mV was determined and subsequently compensated for by the software (115). Cells with leak currents above 100 pA were discarded. In the case of increasing leak currents, the measurement was interrupted, and a new leak compensation was performed using the software so that measurements could be continued. Time courses of whole-cell currents for 500 ms were recorded using a voltage ramp protocol by voltage ramps ranging between -60 and +130 mV every 5 seconds (sweeps). The current density was determined to consider different cell sizes and the corresponding membrane capacities. For the normalization, the current capacity (pA) was divided by the cell membrane capacity (pF) (current density pA/pF).

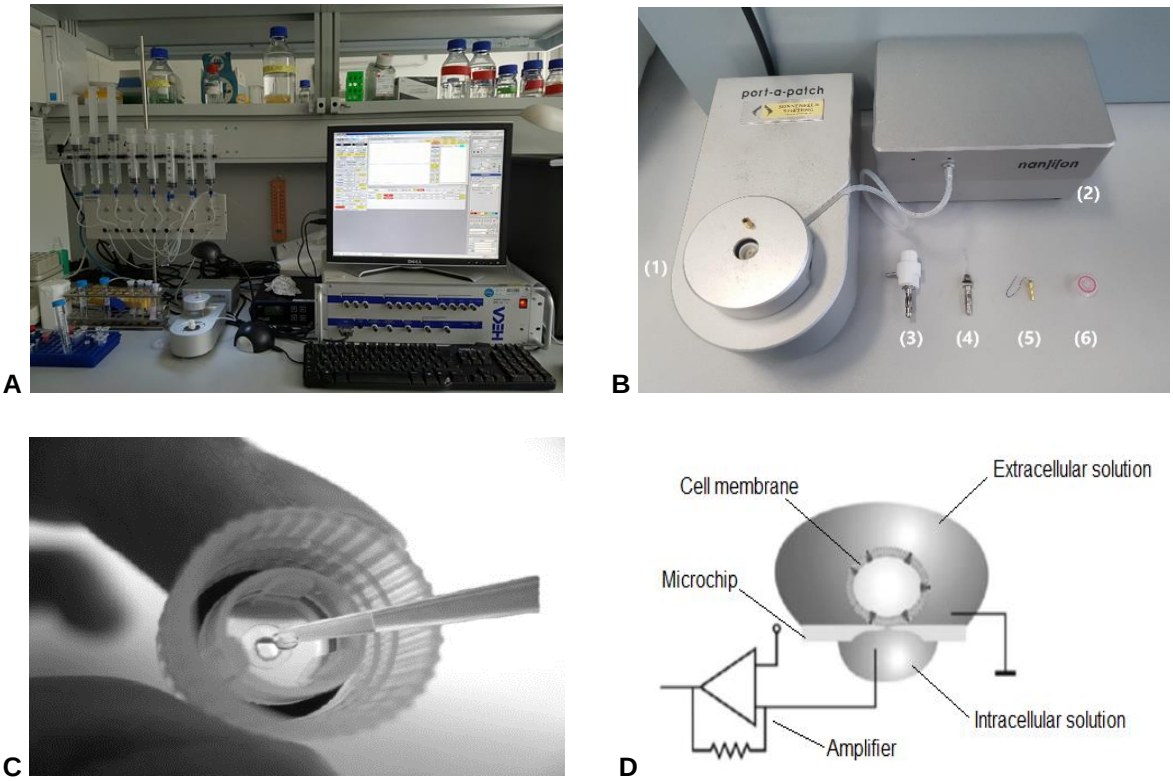

Figure 10: Setup of the planar patch-clamp technique. A: The smallest patch-clamp setup in the world (Port-a-Patch, Nanion, Munich, Germany) was used for this study, located at the Charité University of Medicine – Campus Virchow Clinic, Department of Ophthalmology, Berlin, Germany. The patch-clamp

equipment includes a microchip holder, two electrodes, a pump, an amplifier, and a computer [Image by E. Turan]. **B:** Close-up image of the Port-a-Patch setup: (1) pre-amplifier/ head stage, (2) pump, (3) chip holder, (4) intracellular electrode, (5) extracellular electrode, (6) microchip [Image by E. Turan]. **C:** Close-up image of the microchip [Bruggemann et al. (113)]. The internal solution is applied to the inside of the patch-clamp chip. **D:** Simplified illustration of the microchip technology [modified after Bruggemann et al. (113)].

2.5 Statistical analysis

Excel (Microsoft 2010) was used for the evaluation of the first raw data. All plots were generated using SigmaPlot software version 12.3 (Systat Software, San Jose, California, USA) connected with an electrophysiology module (Systat, Bruxton). Bar charts and statistical analyses were plotted with GraphPad Prism version 5. The parametric Student's t-test for paired data (p-values: two-tailed) was used if all data passed normality tests (D'Agostino and Pearson; Shapiro-Wilk; KS). Otherwise, nonparametric tests were used (Wilcoxon matched paired tests for paired data or Mann-Whitney for unpaired data). The values (error bars) shown in the graphs are ± SEM in both directions and probabilities of $p < 0.05$ (*) were considered as significant (level of significance 5 %). The number of repetitions (n) is shown in brackets next to the bars or mean traces.

3. Results

3.1 Cell morphology of HCK

In this study, a cell model of HCK was used (designated HCK), which was established by Zorn-Kruppa et al. (104). HCK are highly specialized corneal fibroblasts. Therefore, their morphological characteristics are comparable with fibroblasts. Specifically, they express a flattened phenotype with a prominent nucleus. Depending on the current cell density, their cell structure and morphology change (Fig. 11). On the first day of cell culturing, the HCK cells used for this study appear as small round cells isolated from each other. Over the course of few days, the HCK cells show a more elongated shape and semiconfluent cell growth in smaller groups. They exhibit branches, leading to networks of connecting cells (Fig. 16A). During their exponential growth, the cell density increases and the cells transform into a rounder phenotype. If the cells are migrating, they arrange themselves again into parallel elongated shapes (Fig. 16B).

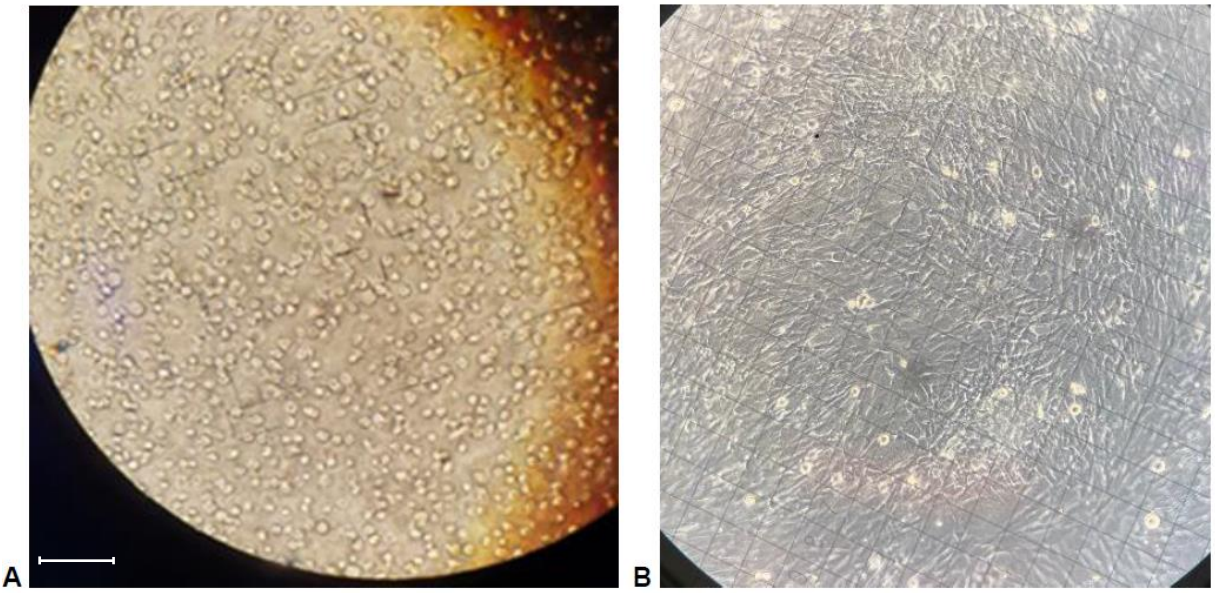

Figure 11: Light microscopic image of a HCK cell suspension. A: Recently prepared HCK cells. Image taken on the first day of cell culturing; scale bar = 200 µm [image by E. Turan]. **B:** HCK cells at higher density. Photo taken on day 3 of cell culturing; grid distance = 100 µm [image kindly provided by Mergler et al.]. For measuring, the cells should have a final confluence of 60 – 80 %, which was approximately assessed under a light microscope.

3.2 Calcium Imaging measurement results in HCK

3.2.1 L-carnitine reduces heat-induced TRPV1 activation

At first, heat > 43 °C was used to activate TRPV1. After heating, a transient increase of f_{340nm}/f_{380nm} from 0.1002 ± 0.0003 (100 s) to 0.1971 ± 0.0068 (300 s) ($p < 0.0001$, n = 205) was achieved (Fig. 12A). To investigate the L-carnitine effect, the prior experiments were repeated in the presence of 1 mM L-carnitine. As a result, the f_{340nm}/f_{380nm} ratio only increased from 0.09827 ± 0.0004 (100 s) to 0.1289 ± 0.0047 (300 s) ($p < 0.0001$, n = 33) (Fig. 12B). Therefore, a heat-induced Ca^{2+} increase was clearly suppressed by L-carnitine (from 0.1971 ± 0.0068 to 0.1289 ± 0.0047, $p < 0.0001$) (Fig. 12C).

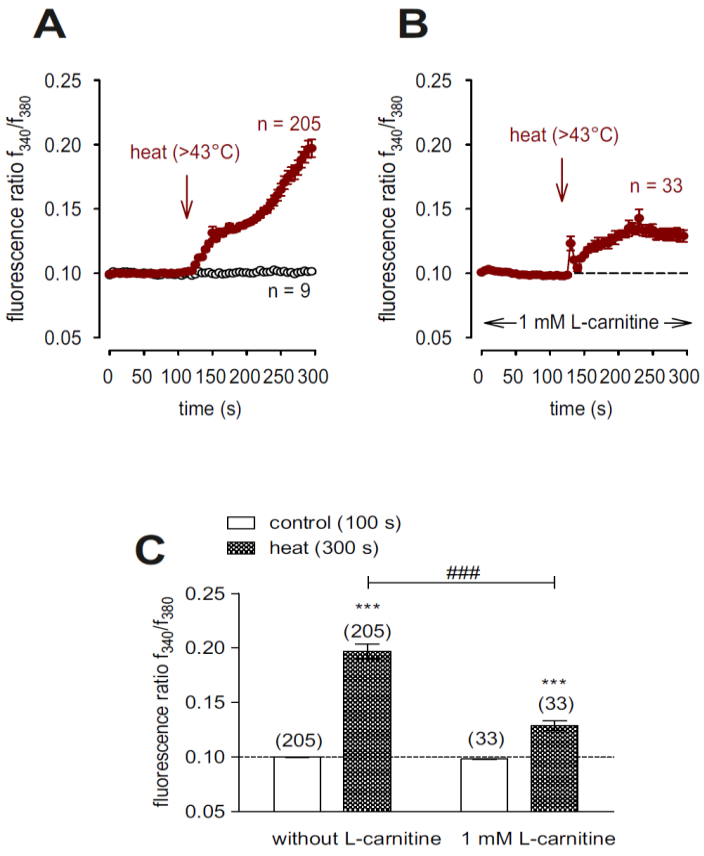

Figure 12: L-carnitine reduces heat-induced increases of intracellular Ca^{2+} concentration in HCK. **A:** Constant Ca^{2+} baseline of non-treated control cells (n = 9). Heating above 43 °C induces an increase in Ca^{2+} influx (n = 205). **B:** The same experiment as shown in (A), but in the presence of 1 mM L-carnitine. L-carnitine reduces the heat-induced Ca^{2+} increase (n = 33). **C:** Summary of the experiments with heat in presence of vs. without L-carnitine. The asterisks (*) represent significant increases in $[Ca^{2+}]_i$ with heat (t = 300 s; n = 205; $p < 0.0001$; paired tested) compared to control (t = 100 s, n = 205). The hashtags (#) designate statistically significant differences in the f_{340nm}/f_{380nm} ratio between heat without and with L-carnitine (t = 300 s; n = 33 - 205; $p < 0.0001$; non-paired tested). [Turan et al. (103)].

3.2.2 L-carnitine reduces hypertonic-induced TRPV1 activation

The same experiment was repeated with a hypertonic solution of 450 mOsM to activate TRPV1, based on an increase of the f_{340nm}/f_{380nm} ratio. More specifically, the f_{340nm}/f_{380nm} ratio increased from 0.1002 ± 0.0001 (100 s) to 0.1105 ± 0.0014 (300 s) ($p < 0.0001$, n = 55) (Fig. 13A). Additionally, an inhibitory effect of L-carnitine was also clearly demonstrated on hypertonic-induced Ca^{2+} influx. While the hypertonic challenge without L-carnitine increased, the f_{340nm}/f_{380nm} ratio in the presence of 1 mM L-carnitine remained nearly unchanged, since its values varied from 0.1001 ± 0.0001 (100 s) to 0.09983 ± 0.0003 (300 s) (n = 73) (Fig. 13B). All in all, the f_{340nm}/f_{380nm} ratio transiently declined from 0.1105 ± 0.0014 to 0.09983 ± 0.0003 ($p < 0.0001$) (Fig. 13C).

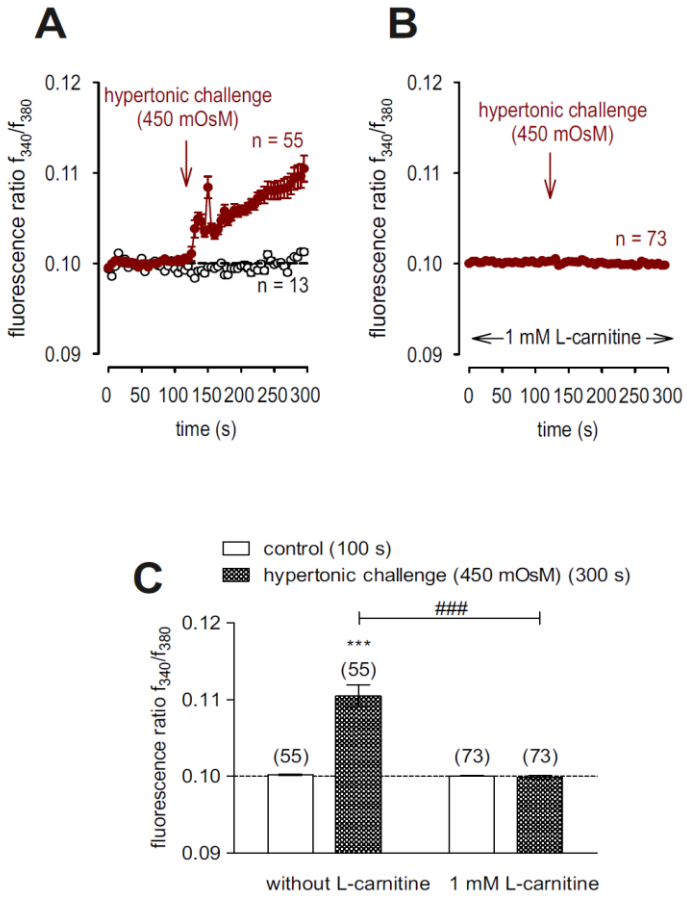

Figure 13: L-carnitine reduces hypertonic-induced increases of intracellular Ca^{2+} concentration in HCK. A: Constant Ca^{2+} baseline of non-treated control cells (n = 13). Hypertonic challenge (450 mOsM) induces an increase in Ca^{2+} influx (n = 55). **B:** The same experiment as shown in (A), but in the presence of 1mM L-carnitine. L-carnitine distinctly suppresses the hypertonic-induced Ca^{2+} increase (n = 73). **C:** Summary of the experiments with hypertonicity in the presence of vs. without L-carnitine. The asterisks (*) show significant increases in $[Ca^{2+}]_i$ with hypertonicity (t = 300 s; n = 55; $p < 0.0001$; paired tested) compared to control (t = 100 s, n = 55). The hashtags (#) designate statistically significant differences in the f_{340nm}/f_{380nm} ratio between hypertonic challenge without and with L-carnitine (t = 300 s; n = 55 - 73; $p < 0.0001$; non-paired tested). [Turan et al. (103)].

3.2.3 L-carnitine reduces CAP-induced TRPV1 activation

Finally, the effect of CAP on TRPV1 activity was evaluated. Consequently, 10 µM CAP also clearly increased the f_{340nm}/f_{380nm} ratio from 0.1004 ± 0.0001 (100 s) to 0.1161 ± 0.0031 (270 s) ($p < 0.0001$, n = 55) (Fig. 14A). Furthermore, L-carnitine had a similar inhibitory effect on CAP-induced TRPV1 activation. In HCK cells preincubated with 1 mM L-carnitine, 10 µM CAP failed to induce a sizable Ca^{2+} transient. Specifically, the f_{340nm}/f_{380nm} ratio slightly increased from 0.09935 ± 0.0002 (100 s) to 0.1006 ± 0.0002 (270 s) (n = 55) (Fig. 14B). In addition, the L-carnitine induced effect on CAP was at significantly lower levels compared to the measurements undertaken without L-carnitine (0.1161 ± 0.0031 vs. 0.1006 ± 0.0002, $p < 0.0001$, n = 55) (Fig. 14C).

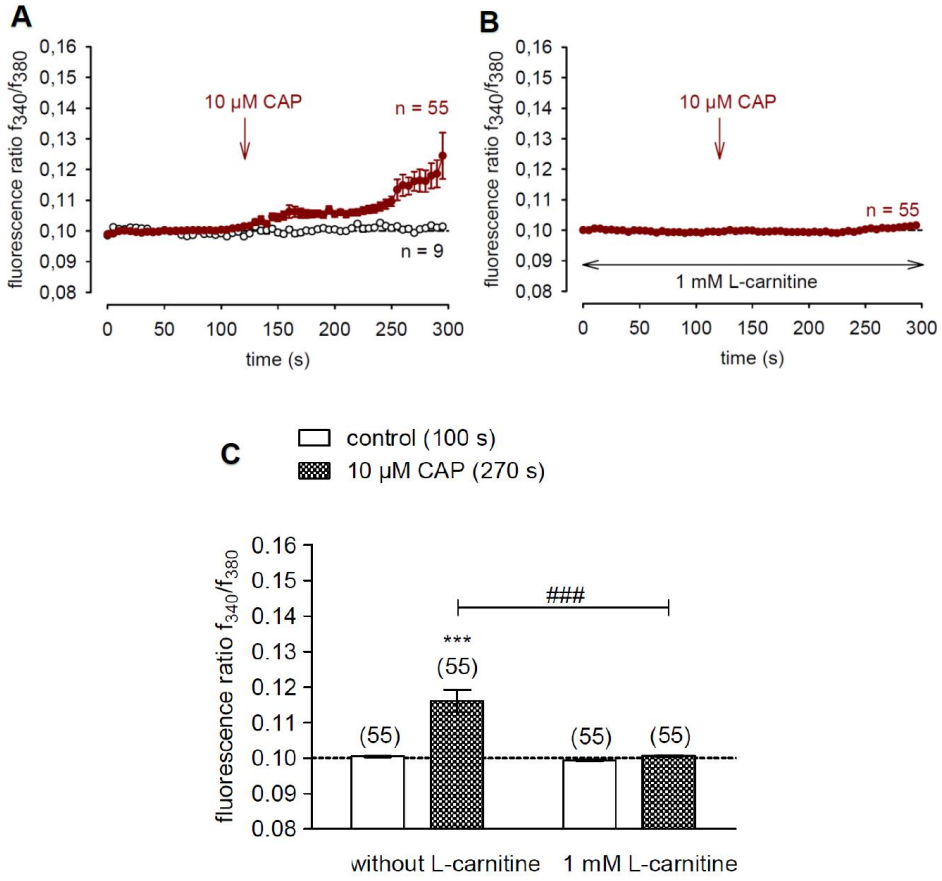

Figure 14: L-carnitine reduces CAP-induced increases of intracellular Ca^{2+} concentration in HCK. **A:** Constant Ca^{2+} baseline of non-treated control cells (n = 9). 10 µM CAP induces an increase in Ca^{2+} influx (n = 55). **B:** The same experiment as shown in (A), but in the presence of 1 mM L-carnitine. L-carnitine distinctly suppresses the CAP-induced Ca^{2+} increase (n = 55). **C:** Summary of the experiments with CAP in the presence of vs. without L-carnitine. The asterisks (*) designate significant increases in $[Ca^{2+}]_i$ with CAP (t = 270 s; n = 55; $p < 0.0001$; paired tested) compared to control (t = 100 s, n = 55). The hashtags (#) show statistically significant differences in the f_{340nm}/f_{380nm} ratio between CAP without and with L-carnitine (t = 270 s; n = 55 - 55; $p < 0.0001$; non-paired tested). [Modified after Turker et al. (111)].

3.3 Planar patch-clamp measurement results in HCK

To ascertain whether there is a correspondence between calcium imaging data and underlying ionic currents measured with the planar patch-clamp procedure, the corresponding effects of CAP were evaluated in the presence and absence of carnitine on whole-cell current behavior in HCK (Fig. 15).

3.3.1 CAP increases whole-cell currents

Whole-cell currents were determined by measuring time-dependent current changes and evaluating the plots of the corresponding current voltage relationships at the labeled time points: A, B and C (Figs. 15A, 15B). At negative potentials of -60 mV, 10 µM CAP increased the inward currents from -11 ± 4 pA/pF to -32 ± 13 pA/pF (n = 7) (Fig. 15C). Similarly, the voltage step from 0 mV to -60 mV increased the maximal inward current amplitudes to -66 ± 32 % of control (control set to 100 %) (n = 7, $p < 0.005$) (Fig. 15D). The same applies to the outward currents at positive potentials of +130 mV. CAP (10 µM) activated typical TRPV1-like outwardly rectifying currents (Fig. 15B). More specifically, the outward currents significantly rose from 172 ± 71 pA/pF to 281 ± 117 pA/pF (n = 7, $p < 0.05$) (Fig. 15C). Additionally, the maximal outward current amplitudes induced by a voltage step from 0 mV to +130 mV increased to 173 ± 13 % of control (control set to 100 %) (n = 7, $p < 0.01$) (Fig. 15E). The reversal potential was continuously around 0 mV, which is indicative of non-selective ion channel behavior. In conclusion, the functional expression of TRPV1 in immortalized HCK cells was confirmed, which is in line with a previous study (103, 111).

3.3.2 L-carnitine reduces CAP-induced whole-cell currents

As shown in Figure 15, L-carnitine suppressed CAP-induced increases of whole-cell currents, which are elicited by a voltage step from -60 mV to +130 mV. CAP (10 µM) increased both the in- and outwardly rectifying currents, whereas these currents were suppressed in the presence of 1 mM L-carnitine (n = 7, $p < 0.05$) (Fig. 15A, 15B, 15C). More specifically, inward current density was significantly suppressed from -32 ± 13 pA/pF to -11 ± 6 pA/pF (n = 7, $p < 0.05$), as was the case in outward current density

which was suppressed from 281 ± 117 pA/pF to 225 ± 109 pA/pF (n = 7, p < 0.05) (Fig. 15C). Furthermore, the maximal inward current amplitudes significantly decreased to 112 ± 16 % of control (control set to 100 %) (n = 7, p < 0.005), induced by a voltage step from 0 mV to -60 mV (Fig. 15D). The maximal outward current amplitudes induced by a voltage step from 0 mV to +130 mV significantly declined to 108 ± 12 % of control (control set to 100 %) (n = 7, p < 0.01) (Fig. 15E). Overall, L-carnitine had a corresponding inhibitory effect on both TRPV1-induced whole-cell currents and increases in intracellular Ca^{2+} levels in HCK.

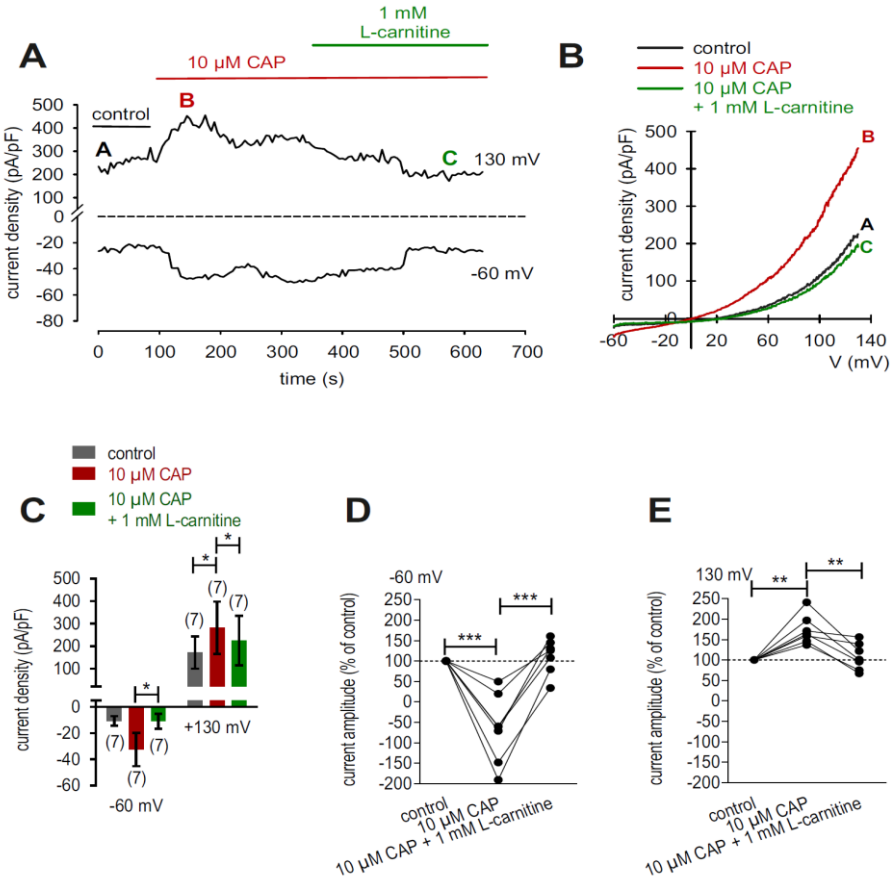

Figure 15: L-carnitine reduces CAP-induced increases of whole-cell currents in HCK. A: Time course recording of the currents. 10 µM CAP induces current increases, whereas application of 1 mM L-carnitine suppresses the current increase. **B:** Original traces of current responses to voltage ramps shown before application (labeled as A), during application of 10 µM CAP (labeled as B), and after adding 1 mM L-carnitine (labeled as C). **C:** Summary of the patch-clamp experiments with CAP in the presence of vs. without L-carnitine. The asterisks (*) designate statistically significant differences of CAP-induced increases of whole-cell currents without and with L-carnitine (n = 7, p < 0.05; paired tested). **D:** Maximal inward current amplitudes induced by a voltage step from 0 mV to -60 mV are shown as percentage of control values before application of 10 µM CAP (control set to 100 %). 1 mM L-carnitine clearly suppressed CAP-induced inward currents. **E:** The same diagram as shown in (D), but related to maximal outward current amplitudes induced by a voltage step from 0 mV to +130 mV. [Turan et al. (103), modified after Turker et al. (111)].

4. Discussion

4.1 Analysis of HCK cell morphology

The HCK cells used for this study stem from a SV40-immortalised keratocyte cell line (named HCK) isolated from human eye bank donor material (104). Zorn-Kruppa et al. established a three-dimensional human corneal equivalent construct, which serves as an *in vitro* model for eye irritation, toxicity, and drug efficacy testing (104). In contrast to primary human cells, HCK cells via S40 transfection have a permanent lifetime without any significant differences in morphology and proliferative behavior to those displayed by non-transformed cells (104). Therefore, they represent an appropriate research tool for the ophthalmic science community (104). Since this cell line expresses typical biomarkers of primary cultures of HCK (111), the results obtained with the immortalized HCK cells have physiological relevance. Notably, in a scratch wound assay, the cells lose their close formation and transform into a more elongated shape as they migrate and reconnect with other cells (Fig. 16). Accordingly, these observations of their migratory behavior reflect their important role in mediating the wound healing response to injury.

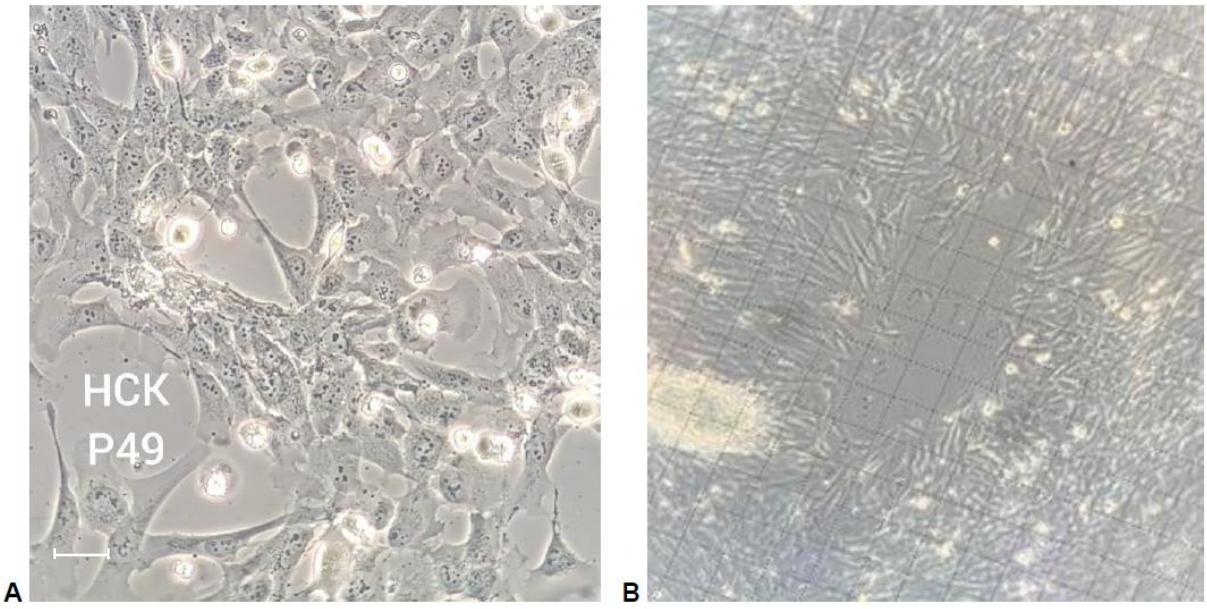

Figure 16: Growth pattern of SV40-immortalized HCK cells. A: HCK cell suspension at lower density showing morphology and growth behavior of HCK cells, passage 49; scale bar = 50 µm. **B:** Scratch-assay showing form formation and cell migration of HCK cells; grid distance = 100 µm. [Images kindly provided by Mergler et al.].

4.2 TRPV1 expression and functional relevance

At present, there are clear indications that TRPV1 has a pathophysiological significance not only in dry eyes (116) but also in responding to a corneal injury (117) and other connected diseases, e.g., with diabetes (118). Specifically, the cell type in which TRPV1 is expressed is crucial. In general, TRPV1 is typically expressed in excitable cells such as in neurons of corneal nerve fibers since TRPV1 is a heat and pain receptor (119). Notably, the cornea is the most sensitive human tissue of the human body with 7000 pain receptors per mm^2 in its nerve fibers, which is 300 – 600 times larger than the receptor density in the dermis (10). In contrast, TRPV1 is also expressed in corneal epithelial cells and fibroblasts, which are in close proximity to the corneal nerves (68). Notably, the functional expression of TRPV1 in HCK was confirmed in this thesis based on responses known to be induced by TRPV1 activation.

At first, heat was used to activate temperature sensitive TRPs (thermo-TRPs) as described in a previous study of HCK (111). Firstly, the Ca^{2+} influx increased by raising the temperature above 43 °C (Fig. 12A), which corresponds to TRPV1 activation as shown in human corneal epithelial cells (HCEC) (68). Despite the fact that under physiological circumstances, temperatures around this range do not occur in the human cornea, 43 °C is the temperature threshold for activating TRPV1 and evoking pain sensation (55, 63). The heat induced Ca^{2+} transients are similar to those measured in human corneal endothelial cells (HCEC-12) (51) as well as epithelial cells (68). Compared with studies investigating functional expression in immortalized pterygial epithelial cells (hPtEC), inducing TRPV1 activation by a thermal stress led to a continuously larger intracellular Ca^{2+} increase than in HCEC or HCK and showed a lack of recovery (120). This difference in Ca^{2+} response suggests a possible association between hyperplastic or cancerous tissue and increases in functional TRPV1 activity as a consequence of increased Ca^{2+} influx (120). Since TRPV1 activation also maintained inflammation response through the MAPK signaling pathway (81, 121), its modulation may be a potential drug target to suppress inflammatory as well as proliferative processes.

Secondly, another possibility to activate TRPV1 is to use hypertonicity, which has been demonstrated in HCEC (67). Notably, the same phenomenon was also observed in HCK. Specifically, exposure to a hyperosmotic solution of 450 mOsM raised the Ca^{2+} influx in HCK (Fig. 13A) similarly to measurements performed in HCjEC (69). Since the

stroma is not directly connected with an increased osmolarity of the tear film inducing TRPV1 activation in connection with dry eyes (116), the role of this kind of activation mechanism in HCK remains so far unknown. Therefore, two parameters are relevant, namely pain processing in corneal nerves and the putative release of pro-inflammatory cytokines in the stroma. Viewed clinically, this may be relevant if the corneal epithelium is fully damaged (e.g., after corneal injuries, epithelial ulceration, herpetic infection).

Finally, TRPV1 can also be pharmacologically activated by CAP (122), as shown in human corneal fibroblasts (HCF) (123) and HCK (111) (Fig. 14A), which is comparable with the CAP-induced Ca^{2+} response in HCEC (81). A similar study using human corneal endothelial cells (HCEC-12) with 20 µM CAP led to larger Ca^{2+} transients than in HCK (51). Here, the concentration of CAP may be a responsible factor for the various increases, since Lucius et al. demonstrated that 20 µM CAP induced a larger Ca^{2+} influx than 5 µM CAP (124).

Furthermore, this study showed that CAP had corresponding stimulatory effects on the whole-cell currents and rises in intracellular Ca^{2+} levels in HCK (Fig. 15). Similar agreements were reported in other ocular cell types like HCEC (68, 81), HCEC-12 (51), HCjEC (69, 120), HCF (123), and hPtEC (120). TRPV1-like currents are non-selective ion channels with an outwardly rectifying current component and a reverse potential of 0 mV (112). The CAP-induced inward currents represent the Ca^{2+} influx, which is attributable to a Ca^{2+} free internal solution and a high Ca^{2+} concentration in the external solution establishing a large inward-directed Ca^{2+} electrochemical gradient. This assumption can be affirmed, since CAP is a highly specific activator of TRPV1 (122), which is a non-selective cation channel (122) and CAP-increased currents persisted even though chloride (Cl^-) was replaced by gluconate (68). The small outward currents under control conditions are probably anion channel currents (Cl^- currents).

Overall, functional TRPV1 expression in HCK was clearly demonstrated in this thesis, which is in line with the aforementioned *in vitro* electrophysiological studies in ocular surface cells (reviewed in (52)). In 2015, an isoform of TRPV1, the so called deltaN-TRPV1, was identified in the brains of osmoregulating vertebrates (125). Furthermore, this TRPV1 channel subtype is different than the one identified in this study, since CAP always led to a clear TRPV1 activation response in HCK, whereas in the brain, CAP failed to induce a Ca^{2+} transient (125). This difference suggests that the deltaN-TRPV1 channel is not expressed in HCK.

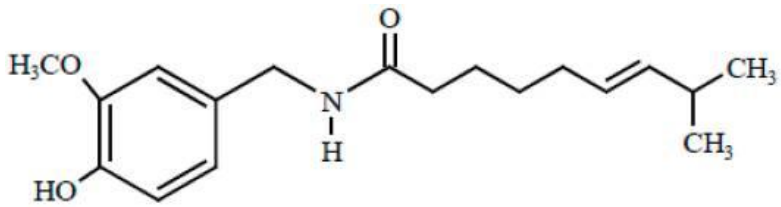

Figure 17: Chemical structure of CAP. CAP is a relatively hydrophobic alkaloid and the main active ingredient of chili peppers (126). It can specifically activate the heat-sensitive TRPV1 ion channel by bonding at the helices S2-S4 (127). Therefore, pure capsaicin is a highly pungent irritant for mammals and causes a sensation of pain and burning. The CAP molecule can be divided into three functional groups: substituted aromatic head region/vanillyl group, dipolar amide-bond region, and hydrophobic tail region. [Chapa-Oliver et al. (128)].

4.3 Effect of L-carnitine on TRPV1 activity

Since L-carnitine is contained in some artificial eye drops (e.g., Allergan, Optive) and provides symptomatic relief in dry eye patients (98, 129-132), its therapeutic potential has gain increasing attention. Moreover, previous studies have documented that some of the symptomatic relief is caused by L-carnitine inhibiting the hyperosmolarity-induced MAPK signaling pathway (133-136), which leads to proinflammatory cytokine release (67, 81). Although, there are indications that L-carnitine is an osmoprotectant and TRPV1 inhibitor (69, 129-132, 135, 136), the effect of L-carnitine has not been investigated in HCK cells so far. In this study, however, the previous findings of L-carnitine in HCK were also confirmed. Figure 18 illustrates the inhibitory effect of L-carnitine on different TRPV1 channel activation pathways.

Notably, L-carnitine was even able to significantly decrease the TRPV1 activation induced by a temperature rise above 43 °C, which is the typical activation temperature for TRPV1 (57) (Fig. 12B). Heat is a relatively nonspecific factor that also induces denaturation of proteins and catalyzes enzymatic reactions. Nevertheless, L-carnitine was able to suppress at least partially heat-activated TRPV1 (Fig. 12C). Application of eye bandages increases the corneal temperature, consequently leading to pain and changed enzyme activities (137). This partial decline in TRPV1 activity suggests that L-carnitine supplementation may have a protective effect against increases of intracellular Ca^{2+} levels induced by temperature rises in HCK cells.

Furthermore, exposure to L-carnitine inhibited both hypertonic- and CAP-induced rises in Ca^{2+} influx in HCK (Figs. 13B, 14B), in contrast to the measurements performed in HCjEC (69). More specifically, Khajavi and colleagues found that preincubating HCjEC with L-carnitine reversed a rise in $[Ca^{2+}]_i$ below the control level induced by either CAP or hypertonic challenge (69). This phenomenon confirmed L-carnitine involvement in osmotic-induced corneal and conjunctival epithelial shrinkage through its uptake by a Na^+ dependent co-transporter (138). Since the rise of $[Ca^{2+}]_i$ in the presence of L-carnitine remained at a control level in this study, it is possible that L-carnitine did not induce an osmoregulatory response through suppressing TRPV1 function in HCK. Therefore, more studies are necessary to investigate the transport mechanism of L-carnitine in corneal stroma including HCK.

Additionally, L-carnitine also clearly suppressed CAP-induced increases of whole-cell currents in HCK (Fig. 15). This is comparable to those elicited by L-carnitine in HCjEC (69) as well as by the TRPV1 antagonist capsazepine (CPZ) in human uveal melanoma cells (139), HCEC-12 (51), HCF (123), HCjEC (120), and hPtEC (120).

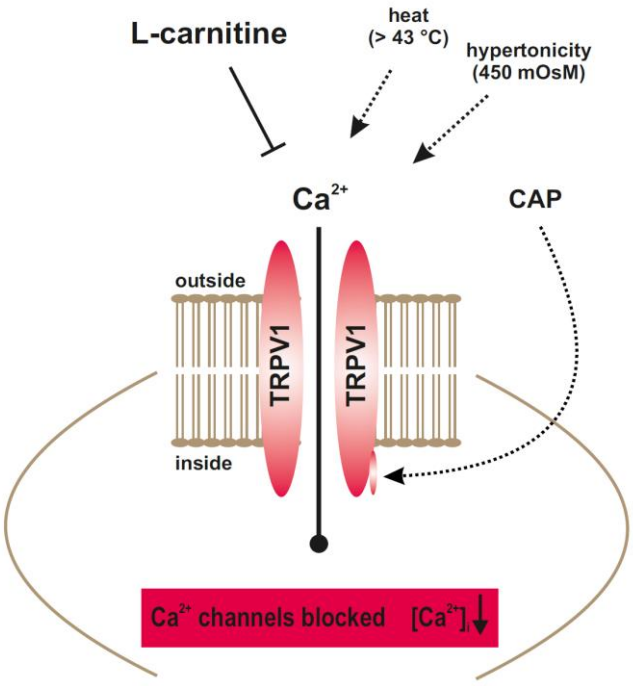

Figure 18: Simplified scheme of the L-carnitine effect on different TRPV1 channel activation pathways. TRPV1 (capsaicin receptor) can be selectively activated by CAP, heat above 43 °C, and hypertonic challenge. All three different TRPV1 activation mechanisms can be suppressed by L-carnitine, which leads overall to reduced intracellular Ca^{2+} concentration. [Image by S. Mergler (103)].

4.4 Clinical relevance and future perspective

Since the cornea has most of the refractive power in the eye, loss of corneal transparency is a leading cause of blindness. Increased tear osmolarity correlates with ocular surface damage and is associated with the inflammation processes demonstrated in *in vitro* HCEC culture models (78, 80, 81, 140), as well as in studies using mice models inducing dry eyes by systemic administration of scopolamine and exposure to an air draft (141-143). Since TRPV1 can be activated by hyperosmolarity and its activation induces inflammatory cytokine release through MAPK signaling pathways (81), this channel fits exactly into the DES pathophysiology. Moreover, increased levels of proinflammatory cytokines (IL-1 and TNFα) as well as MMPs (MMP-3 and -9) have been observed in the tear fluid of DES patients (144-147), which also confirms and supports the exceptional role of TRPV1. Additionally, the MMP family have been recognized as the enzymes involved in further ocular surface diseases including wound healing, corneal ulceration etc. (148-151). Therefore, TRPV1 activation seems to not only affect the corneal epithelium but also deeper tissues including the corneal stroma. In this context, investigations of TRPV1 modulation also plays an important role in corneal stroma cells like HCK. This is why novel promising approaches are being targeted to selectively inhibit injury or infection-induced TRPV1 activity – which otherwise induce inflammation, pain-related symptoms, stromal fibrosis etc. – in order to prevent corneal transparency losses.

One such inhibitory agent is L-carnitine, which may reduce pain processes as well as the release of pro-inflammatory cytokines (129-136). Clinically, carnitine is neuroprotective (152, 153) and has been widely recommended as a supplement to treat cardiovascular and other diseases (154-157). In this context, L-carnitine not only plays a role in preventive medicine, but also in ocular pathologies such as DED (97), cataracts (158) or retinopathy (159). The neuroprotective aspect of L-carnitine may also be beneficial in the pathophysiology of neurotrophic keratopathy (NK). NK is a degenerative corneal disease based on corneal innervation impairment. In 2018, Dua and colleagues released an updated definition of NK, namely: “NK is defined as a disease related to alterations in corneal nerves leading to impairment in sensory and trophic function with consequent breakdown of the corneal epithelium affecting health and integrity of the tear film, epithelium and stroma“ (77). Various factors are able to cause trigeminal nerve damage leading to NK - the most common are herpetic infections (160) and neuro-ophthalmic surgical procedures (161). In the cornea,

epithelial cells and keratocytes secrete neurotrophic factors such as nerve growth factor (NGF) (162), which in turn promotes the regeneration of the corneal nerves (163, 164) and modulates corneal wound healing (165). Due to the fact that the corneal innervation is responsible for corneal epithelial regeneration as well as tear secretion, a disruption in corneal innervation has adverse effects on both functions. While stage 1 (mild) of NK exhibits ocular surface irregularity and vision reduction, stage 2 (moderate) indicates a nonhealing persistent epithelial defect, and stage 3 (severe) shows corneal ulceration involving subepithelial (stromal) tissue, possibly leading to corneal perforation (77). Therefore, further studies are necessary to investigate, on the one hand, the preventive use of L-carnitine (e.g., before/during surgical treatment), and on the other, the therapeutic approach using L-carnitine regarding pain reduction and corneal sensation.

However, additional studies have shown that the conversion of keratocytes and fibroblasts into terminally differentiated myofibroblasts induced by TRPV1 activation results in the obstruction of stromal organization. Consequently, this terminated in normal vision impairment (33, 67, 81, 117, 166, 167). Preliminary studies have shown that blocking TRPV1 suppressed stromal fibroblast transdifferentiation into myofibroblasts as well as TGFβ1 expression in cultured keratocytes or ocular fibroblasts. This demonstrates the importance of TRPV1 function in mediating wound healing processes (82, 166, 168). In this context, studies on the loss of TRPV1 function demonstrated wound healing impairment of stromal incision in mice, based on less alpha-smooth muscle actin (αSMA) upregulation, fewer differentiated myofibroblasts at the wound edge as well as less activated TGFβ expression (82, 166, 168). Additionally, it was shown that L-carnitine slightly decelerated HCK cell migration over a period of 8 hours and delayed wound closure after 24 hours, which supports the inhibitory effect of L-carnitine on TRPV1 (103).

Apart from *in vitro* studies showing a link between L-carnitine and TRPV1 (69, 103, 111), there are no clinical studies focusing on the effect of L-carnitine either in concomitant TRPV1 silencing or the suppression of TRPV1-induced release of proinflammatory cytokines. Certainly, L-carnitine is not the only agent with an antagonistic TRPV1 function. There are also other possibilities to inhibit TRPV1 activation, which may be developed for therapeutic use. TRPM8, also known as menthol or cold receptor, which can be activated by thyronamine ($3T_1AM$) or Borneol,

is able to inhibit TRPV1 through crosstalk (124, 169-172). Therefore, further studies are necessary to characterize the functions of these agents more specifically and also regarding their interactions as well as side effects. For example, Borneol is known to have adverse effects in the mouse brain (116).

All these findings affirm the estimation that L-carnitine may be an important therapeutic agent for improving the outcome of inflammatory and fibrogenic wound healing through TRPV1 suppression in HCK. Therefore, further clinical studies are necessary to investigate the clinical application of L-carnitine into the different corneal layers as well as L-carnitine transporters into deeper corneal cell layers in the stroma and the endothelium.

4.5 Limitations

4.5.1 Cell culture handling

Despite the fact that the longevity of suspended cells can be improved by careful handling, the cell preparation was performed under non-physiological conditions. The experiments took place at room temperature, whilst according to the manufacturer Nanion's guidelines, HCK cells achieve their optimal activity at 37 °C, 95 % humidity and 5 % CO_2 (113, 114). Instead of trypsin, as described in the guidelines, accutase was used for detaching the cells from the flask surface. In contrast to trypsin, which may damage the cell membrane if the incubation time is too long, accutase is self-digesting and does not significantly affect the proliferation and viability rate of the cells (173). Additionally, the cells were exposed to environmental influences, for example changing temperatures (from the incubator to room temperature) or mechanical stress because of pipetting. Therefore, every step of the cell handling could have stressed the cells and affected the measurements. Damaged or dead cells could not be fully excluded during the measurements. This can affect the results and also has to be considered. Lastly, there is a relevant disparity between *in vitro* and *in vivo* conditions. Cell cultures are a simplified representation of reality, whereby the exactness of a simulation of physiological *in vivo* conditions is limited. On the other hand, the cultured HCK cells represent an established cell culture model from a SV40-immortalised corneal cell line (104). Irrespective of that, hypertonic and CAP-induced TRPV1

activation was demonstrated at different cell passages (data not shown), indicating a stable cell line.

4.5.2 Technical limitations

The rapid progress in the technical development of established measuring methods such as fluorescence calcium imaging and patch-clamp technique has rapidly improved over the years. However, their limited informative value has to be considered and discussed. Despite the highly sensitive functionality of these measures, relatively high data scattering occurred, due to a more or less poor signal-to-noise ratio. Despite creating equal framework conditions for all calcium imaging measurements, slight growth differences and measuring variations occurred in the baselines. On the one hand, cell stress can be caused by the adaptation of the cells to room temperature and on the other, by the transport into the coverslips as well the pipetting procedure. Furthermore, spontaneous Ca^{2+} release from intracellular organelles such as endoplasmic reticulum induced spikes during the measuring of the baseline. Some bleaching problems during the calcium imaging measurements were more or less compensated for by the TIDA software for drift correction.

In this thesis, the semi-automated planar patch-clamp technique described by Bruggemann et al. in 2006 was used instead of the conventional patch-clamp technique described by Hamill in 1981 (174) (Fig. 19). In contrast to the conventional patch-clamp, where the pipette penetrates into the cell, a software-controlled pump draws a single cell to a microchip opening. This chip has a micro-opening of ≈ 1 – 3 µm and a resistance of 3 – 5 MΩ, which was required for the recordings. The resistance of the microchip corresponded to that of a patch pipette for whole-cell recordings. Whilst the conventional method requires experimental skills, the planar patch-clamp technique overcomes these limitations. Nonetheless, even the modernized planar patch-clamp device has some limitations. Leak currents were a regularly occurring interfering factor. They can occur at high levels, when the cell is not well-connected on the microchip, and can negatively influence the ion channel currents. Although the leak currents were compensated for by the PatchControl software, several seal problems occurred because these currents can change during the measurement. Recordings with unstable seals and leak currents above 100 pA were discarded from the data

evaluation. Another limiting factor was resistance series (Rs) values of above 30 MOhm caused by a blocked microchip-opening.

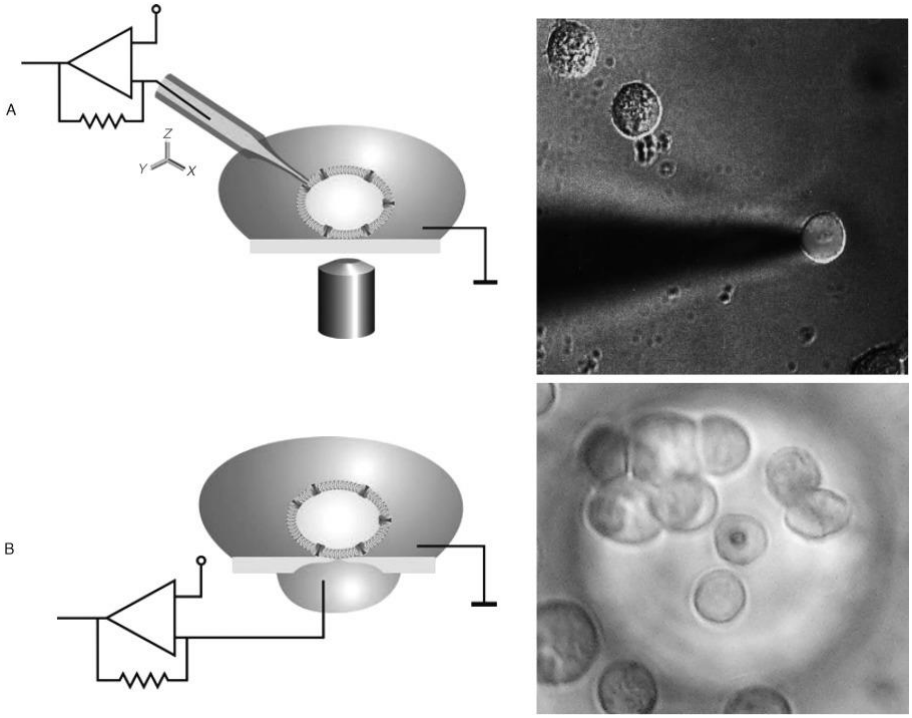

Figure 19: Simplified presentation of classical and planar patch-clamp technique. (A) Schematic and microscopy image of the conventional patch-clamp technique. The tip of the glass pipette is filled with electrolyte solution and is positioned on a cell using an x,y,z micromanipulator and a binocular microscope. (B) Schematic and microscopy image of the semiautomated planar patch-clamp technique. Cells in suspension are positioned onto the aperture by a software-controlled application of suction. Neither microscope nor micromanipulator are needed. [Bruggemann et al. (113)].

Interestingly, there are outward currents under control conditions indicating that there are active ion channels. This may be TRPs, since they are at least partially active at room temperature. However, anion channel currents could not be excluded. Specifically, these currents were most likely induced by negative ions such as Cl^- contained in both intra- and extracellular solutions. However, similar studies on HCEC revealed that a replacement of sodium chloride by sodium gluconate did not change the outward current amplitudes, suggesting that any Cl^- currents are probably also insignificant in HCK (68).

Despite the aforementioned confounding factors, the numerous repetitions of the experiments show a clear and significant tendency, which were similar to other studies using L-carnitine as a TRPV1 inhibitor (69, 103, 111).

References

1. Rufer F, Schroder A, Erb C. White-to-white corneal diameter: normal values in healthy humans obtained with the Orbscan II topography system. Cornea. 2005;24(3):259-61.
2. Patel S, McLaren J, Hodge D, Bourne W. Normal human keratocyte density and corneal thickness measurement by using confocal microscopy in vivo. Invest Ophthalmol Vis Sci. 2001;42(2):333-9.
3. Erie JC, Patel SV, McLaren JW, Ramirez M, Hodge DO, Maguire LJ, Bourne WM. Effect of myopic laser in situ keratomileusis on epithelial and stromal thickness: a confocal microscopy study. Ophthalmology. 2002;109(8):1447-52.
4. Reinstein DZ, Archer TJ, Gobbe M, Silverman RH, Coleman DJ. Stromal thickness in the normal cornea: three-dimensional display with artemis very high-frequency digital ultrasound. J Refract Surg. 2009;25(9):776-86.
5. Waring GO, 3rd, Bourne WM, Edelhauser HF, Kenyon KR. The corneal endothelium. Normal and pathologic structure and function. Ophthalmology. 1982;89(6):531-90.
6. Johnson DH, Bourne WM, Campbell RJ. The ultrastructure of Descemet's membrane. I. Changes with age in normal corneas. Arch Ophthalmol. 1982;100(12):1942-7.
7. Dua HS, Faraj LA, Said DG, Gray T, Lowe J. Human corneal anatomy redefined: a novel pre-Descemet's layer (Dua's layer). Ophthalmology. 2013;120(9):1778-85.
8. Mergler S, Valtink M, Takayoshi S, Okada Y, Miyajima M, Saika S, Reinach PS. Temperature-sensitive transient receptor potential channels in corneal tissue layers and cells. Ophthalmic Res. 2014;52(3):151-9.
9. Secker GA, Daniels JT. Limbal epithelial stem cells of the cornea. StemBook. Cambridge (MA)2008.
10. Muller LJ, Marfurt CF, Kruse F, Tervo TM. Corneal nerves: structure, contents and function. Exp Eye Res. 2003;76(5):521-42.
11. Muller LJ, Pels L, Vrensen GF. Ultrastructural organization of human corneal nerves. Invest Ophthalmol Vis Sci. 1996;37(4):476-88.
12. Muller LJ, Pels E, Vrensen GF. The specific architecture of the anterior stroma accounts for maintenance of corneal curvature. Br J Ophthalmol. 2001;85(4):437-43.
13. Schimmelpfennig B. Nerve structures in human central corneal epithelium. Graefes Arch Clin Exp Ophthalmol. 1982;218(1):14-20.
14. Al-Aqaba MA, Fares U, Suleman H, Lowe J, Dua HS. Architecture and distribution of human corneal nerves. Br J Ophthalmol. 2010;94(6):784-9.
15. Srinivasan S, Lyall DA. Neurotrophic Keratopathy. Ocular Surface Disease: Cornea, Conjunctiva and Tear Film: Elsevier; 2013. p. 205-11.
16. Mertsch S, Alder J, Dua HS, Geerling G. [Pathogenesis and epidemiology of neurotrophic keratopathy]. Ophthalmologe. 2019;116(2):109-19.
17. Nishida T. [The cornea: stasis and dynamics]. Nippon Ganka Gakkai Zasshi. 2008;112(3):179-212; discussion 3.
18. Newsome DA, Gross J, Hassell JR. Human corneal stroma contains three distinct collagens. Invest Ophthalmol Vis Sci. 1982;22(3):376-81.
19. Hayashi K, Sueishi K, Tanaka K, Inomata H. Immunohistochemical evidence of the origin of human corneal endothelial cells and keratocytes. Graefes Arch Clin Exp Ophthalmol. 1986;224(5):452-6.
20. Wilson SE, Mohan RR, Mohan RR, Ambrosio R, Jr., Hong J, Lee J. The corneal wound healing response: cytokine-mediated interaction of the epithelium, stroma, and inflammatory cells. Prog Retin Eye Res. 2001;20(5):625-37.
21. Fini ME. Keratocyte and fibroblast phenotypes in the repairing cornea. Prog Retin Eye Res. 1999;18(4):529-51.

22. Jester JV, Moller-Pedersen T, Huang J, Sax CM, Kays WT, Cavangh HD, Petroll WM, Piatigorsky J. The cellular basis of corneal transparency: evidence for 'corneal crystallins'. J Cell Sci. 1999;112 (Pt 5):613-22.
23. West-Mays JA, Dwivedi DJ. The keratocyte: corneal stromal cell with variable repair phenotypes. Int J Biochem Cell Biol. 2006;38(10):1625-31.
24. Fukuda K, Fujitsu Y, Kumagai N, Nishida T. Characterization of the interleukin-4 receptor complex in human corneal fibroblasts. Invest Ophthalmol Vis Sci. 2002;43(1):183-8.
25. Maertzdorf J, Osterhaus AD, Verjans GM. IL-17 expression in human herpetic stromal keratitis: modulatory effects on chemokine production by corneal fibroblasts. J Immunol. 2002;169(10):5897-903.
26. Joseph A, Hossain P, Jham S, Jones RE, Tighe P, McIntosh RS, Dua HS. Expression of CD34 and L-selectin on human corneal keratocytes. Invest Ophthalmol Vis Sci. 2003;44(11):4689-92.
27. Gipson IK. The ocular surface: the challenge to enable and protect vision: the Friedenwald lecture. Invest Ophthalmol Vis Sci. 2007;48(10):4390; 1-8.
28. Wilson SL, Yang Y, El Haj AJ. Corneal stromal cell plasticity: in vitro regulation of cell phenotype through cell-cell interactions in a three-dimensional model. Tissue Eng Part A. 2014;20(1-2):225-38.
29. Wilson SE, He YG, Weng J, Li Q, McDowall AW, Vital M, Chwang EL. Epithelial injury induces keratocyte apoptosis: hypothesized role for the interleukin-1 system in the modulation of corneal tissue organization and wound healing. Exp Eye Res. 1996;62(4):325-7.
30. Wilson SE, Pedroza L, Beuerman R, Hill JM. Herpes simplex virus type-1 infection of corneal epithelial cells induces apoptosis of the underlying keratocytes. Exp Eye Res. 1997;64(5):775-9.
31. Mohan RR, Liang Q, Kim WJ, Helena MC, Baerveldt F, Wilson SE. Apoptosis in the cornea: further characterization of Fas/Fas ligand system. Exp Eye Res. 1997;65(4):575-89.
32. Wilson SE, Kim WJ. Keratocyte apoptosis: implications on corneal wound healing, tissue organization, and disease. Invest Ophthalmol Vis Sci. 1998;39(2):220-6.
33. Jester JV, Petroll WM, Cavanagh HD. Corneal stromal wound healing in refractive surgery: the role of myofibroblasts. Prog Retin Eye Res. 1999;18(3):311-56.
34. Mohan RR, Mohan RR, Kim WJ, Wilson SE. Modulation of TNF-alpha-induced apoptosis in corneal fibroblasts by transcription factor NF-kappaB. Invest Ophthalmol Vis Sci. 2000;41(6):1327-36.
35. Stramer BM, Zieske JD, Jung JC, Austin JS, Fini ME. Molecular mechanisms controlling the fibrotic repair phenotype in cornea: implications for surgical outcomes. Invest Ophthalmol Vis Sci. 2003;44(10):4237-46.
36. Wilson SE, Netto M, Ambrosio R, Jr. Corneal cells: chatty in development, homeostasis, wound healing, and disease. Am J Ophthalmol. 2003;136(3):530-6.
37. Kim WJ, Mohan RR, Mohan RR, Wilson SE. Effect of PDGF, IL-1alpha, and BMP2/4 on corneal fibroblast chemotaxis: expression of the platelet-derived growth factor system in the cornea. Invest Ophthalmol Vis Sci. 1999;40(7):1364-72.
38. Cosens DJ, Manning A. Abnormal electroretinogram from a Drosophila mutant. Nature. 1969;224(5216):285-7.
39. Montell C. Physiology, phylogeny, and functions of the TRP superfamily of cation channels. SciSTKE. 2001;2001(90):RE1.
40. Montell C. The TRP superfamily of cation channels. SciSTKE. 2005;2005(272):re3.
41. Nilius B, Owsianik G. The transient receptor potential family of ion channels. Genome Biol. 2011;12(3):218.
42. Hellmich UA, Gaudet R. Structural biology of TRP channels. Handb Exp Pharmacol. 2014;223:963-90.
43. Launay P, Fleig A, Perraud AL, Scharenberg AM, Penner R, Kinet JP. TRPM4 is a Ca2+-activated nonselective cation channel mediating cell membrane depolarization. Cell. 2002;109(3):397-407.
44. Hofmann T, Chubanov V, Gudermann T, Montell C. TRPM5 is a voltage-modulated and Ca(2+)-activated monovalent selective cation channel. Curr Biol. 2003;13(13):1153-8.
45. Clapham DE. TRP channels as cellular sensors. Nature. 2003;426(6966):517-24.

46. Ramsey IS, Delling M, Clapham DE. An introduction to TRP channels. Annu Rev Physiol. 2006;68:619-47.
47. Lang F, Foller M, Lang KS, Lang PA, Ritter M, Gulbins E, Vereninov A, Huber SM. Ion channels in cell proliferation and apoptotic cell death. JMembrBiol. 2005;205(3):147-57.
48. Sappington RM, Sidorova T, Long DJ, Calkins D. TRPV1: Contribution to Retinal Ganglion Cell Apoptosis and Increased Intracellular Ca2+ with Exposure to Hydrostatic Pressure. Investigative Ophthalmology & Visual Science. 2009;50(2):717-28.
49. Orrenius S, Zhivotovsky B, Nicotera P. Regulation of cell death: the calcium-apoptosis link. Nat Rev Mol Cell Biol. 2003;4(7):552-65.
50. Quallo T, Vastani N, Horridge E, Gentry C, Parra A, Moss S, Viana F, Belmonte C, Andersson DA, Bevan S. TRPM8 is a neuronal osmosensor that regulates eye blinking in mice. Nat Commun. 2015;6:7150.
51. Mergler S, Valtink M, Coulson-Thomas VJ, Lindemann D, Reinach PS, Engelmann K, Pleyer U. TRPV channels mediate temperature-sensing in human corneal endothelial cells. Exp Eye Res. 2010;90(6):758-70.
52. Reinach PS, Mergler S, Okada Y, Saika S. Ocular transient receptor potential channel function in health and disease. BMC Ophthalmol. 2015;15 Suppl 1:153.
53. Reinach PS, Chen W, Mergler S. Polymodal roles of transient receptor potential channels in the control of ocular function. Eye Vis (Lond). 2015;2(1):5.
54. Mergler S. Functional expression of temperature-sensitive transient receptor potential channels (TRPs) in cultured human corneal and conjunctival cells: Relevance in the pathophysiology of ocular surface diseases [Habilitation Thesis]. Free University Berlin, URL: http://www.diss.fu-berlin.de/diss/servlets/MCRFileNodeServlet/FUDISS_derivate_000000018082/Mergler_Habilschrift_mit_DOI_Links.pdf: Charité Universitätsmedizin Berlin; 2015. (last access on 30th June 2021)
55. Caterina MJ, Schumacher MA, Tominaga M, Rosen TA, Levine JD, Julius D. The capsaicin receptor: a heat-activated ion channel in the pain pathway. Nature. 1997;389(6653):816-24.
56. Adcock JJ. TRPV1 receptors in sensitisation of cough and pain reflexes. Pulm Pharmacol Ther. 2009;22(2):65-70.
57. Tominaga M, Caterina MJ. Thermosensation and pain. J Neurobiol. 2004;61(1):3-12.
58. Basbaum AI, Bautista DM, Scherrer G, Julius D. Cellular and molecular mechanisms of pain. Cell. 2009;139(2):267-84.
59. Caterina MJ, Leffler A, Malmberg AB, Martin WJ, Trafton J, Petersen-Zeitz KR, Koltzenburg M, Basbaum AI, Julius D. Impaired nociception and pain sensation in mice lacking the capsaicin receptor. Science. 2000;288(5464):306-13.
60. Davis JB, Gray J, Gunthorpe MJ, Hatcher JP, Davey PT, Overend P, Harries MH, Latcham J, Clapham C, Atkinson K, Hughes SA, Rance K, Grau E, Harper AJ, Pugh PL, Rogers DC, Bingham S, Randall A, Sheardown SA. Vanilloid receptor-1 is essential for inflammatory thermal hyperalgesia. Nature. 2000;405(6783):183-7.
61. Chang Z, Okamoto K, Tashiro A, Bereiter DA. Ultraviolet irradiation of the eye and Fos-positive neurons induced in trigeminal brainstem after intravitreal or ocular surface transient receptor potential vanilloid 1 activation. Neuroscience. 2010;170(2):678-85.
62. Acosta MC, Luna C, Quirce S, Belmonte C, Gallar J. Corneal sensory nerve activity in an experimental model of UV keratitis. Invest Ophthalmol Vis Sci. 2014;55(6):3403-12.
63. Tominaga M, Caterina MJ, Malmberg AB, Rosen TA, Gilbert H, Skinner K, Raumann BE, Basbaum AI, Julius D. The cloned capsaicin receptor integrates multiple pain-producing stimuli. Neuron. 1998;21(3):531-43.
64. Siemens J, Zhou S, Piskorowski R, Nikai T, Lumpkin EA, Basbaum AI, King D, Julius D. Spider toxins activate the capsaicin receptor to produce inflammatory pain. Nature. 2006;444(7116):208-12.
65. Ciura S, Bourque CW. Transient receptor potential vanilloid 1 is required for intrinsic osmoreception in organum vasculosum lamina terminalis neurons and for normal thirst responses to systemic hyperosmolality. J Neurosci. 2006;26(35):9069-75.

66. Martinez-Garcia MC, Martinez T, Paneda C, Gallego P, Jimenez AI, Merayo J. Differential expression and localization of transient receptor potential vanilloid 1 in rabbit and human eyes. Histol Histopathol. 2013;28(11):1507-16.
67. Pan Z, Wang Z, Yang H, Zhang F, Reinach PS. TRPV1 activation is required for hypertonicity-stimulated inflammatory cytokine release in human corneal epithelial cells. Invest Ophthalmol Vis Sci. 2011;52(1):485-93.
68. Mergler S, Garreis F, Sahlmuller M, Reinach PS, Paulsen F, Pleyer U. Thermosensitive transient receptor potential channels in human corneal epithelial cells. J Cell Physiol. 2011;226(7):1828-42.
69. Khajavi N, Reinach PS, Skrzypski M, Lude A, Mergler S. L-Carnitine Reduces in Human Conjunctival Epithelial Cells Hypertonic-Induced Shrinkage through Interacting with TRPV1 Channels. Cellular Physiology and Biochemistry. 2014;34(3):790-803.
70. Belmonte C, Acosta MC, Merayo-Lloves J, Gallar J. What Causes Eye Pain? Curr Ophthalmol Rep. 2015;3(2):111-21.
71. Valim V, Trevisani VF, de Sousa JM, Vilela VS, Belfort R, Jr. Current Approach to Dry Eye Disease. Clin Rev Allergy Immunol. 2014.
72. Schaumberg DA, Nichols JJ, Papas EB, Tong L, Uchino M, Nichols KK. The international workshop on meibomian gland dysfunction: report of the subcommittee on the epidemiology of, and associated risk factors for, MGD. Invest Ophthalmol Vis Sci. 2011;52(4):1994-2005.
73. Schein OD, Munoz B, Tielsch JM, Bandeen-Roche K, West S. Prevalence of dry eye among the elderly. Am J Ophthalmol. 1997;124(6):723-8.
74. Posa A, Sel S, Dietz R, Sander R, Brauer L, Paulsen F. [Updated incidence of dry eye syndrome in Germany]. Klin Monbl Augenheilkd. 2014;231(1):42-6.
75. Steven P, Cursiefen C. [Anti-inflammatory treatment in dry eye disease]. Klin Monbl Augenheilkd. 2012;229(5):500-5.
76. Lemp MA, Crews LA, Bron AJ, Foulks GN, Sullivan BD. Distribution of aqueous-deficient and evaporative dry eye in a clinic-based patient cohort: a retrospective study. Cornea. 2012;31(5):472-8.
77. Dua HS, Said DG, Messmer EM, Rolando M, Benitez-Del-Castillo JM, Hossain PN, Shortt AJ, Geerling G, Nubile M, Figueiredo FC, Rauz S, Mastropasqua L, Rama P, Baudouin C. Neurotrophic keratopathy. Prog Retin Eye Res. 2018;66:107-31.
78. The definition and classification of dry eye disease: report of the Definition and Classification Subcommittee of the International Dry Eye WorkShop (2007). Ocul Surf. 2007;5(2):75-92.
79. Tomlinson A, Khanal S, Ramaesh K, Diaper C, McFadyen A. Tear film osmolarity: determination of a referent for dry eye diagnosis. Invest Ophthalmol Vis Sci. 2006;47(10):4309-15.
80. Igarashi T, Fujimoto C, Suzuki H, Ono M, Iijima O, Takahashi H, Takahashi H. Short-time exposure of hyperosmolarity triggers interleukin-6 expression in corneal epithelial cells. Cornea. 2014;33(12):1342-7.
81. Zhang F, Yang H, Wang Z, Mergler S, Liu H, Kawakita T, Tachado SD, Pan Z, Capo-Aponte JE, Pleyer U, Koziel H, Kao WW, Reinach PS. Transient receptor potential vanilloid 1 activation induces inflammatory cytokine release in corneal epithelium through MAPK signaling. J Cell Physiol. 2007;213(3):730-9.
82. Nidegawa-Saitoh Y, Sumioka T, Okada Y, Reinach PS, Flanders KC, Liu CY, Yamanaka O, Kao WW, Saika S. Impaired healing of cornea incision injury in a TRPV1-deficient mouse. Cell Tissue Res. 2018;374(2):329-38.
83. Sumioka T, Okada Y, Reinach PS, Shirai K, Miyajima M, Yamanaka O, Saika S. Impairment of corneal epithelial wound healing in a TRPV1-deficient mouse. Invest Ophthalmol Vis Sci. 2014;55(5):3295-302.
84. Fraenkel G, Friedman S. Carnitine. Vitam Horm. 1957;15:73-118.
85. Bremer J. Biosynthesis of carnitine in vivo. Biochimica et Biophysica Acta. 1961;48(3):622-4.
86. Wolf G, Berger CR. Studies on the biosynthesis and turnover of carnitine. Arch Biochem Biophys. 1961;92:360-5.
87. Tanphaichitr V, Broquist HP. Role of lysine and -N-trimethyllysine in carnitine biosynthesis. II. Studies in the rat. J Biol Chem. 1973;248(6):2176-81.

88. Pettegrew JW, Levine J, McClure RJ. Acetyl-L-carnitine physical-chemical, metabolic, and therapeutic properties: relevance for its mode of action in Alzheimer's disease and geriatric depression. Mol Psychiatry. 2000;5(6):616-32.
89. Friedman S, Fraenkel G. Reversible enzymatic acetylation of carnitine. Arch Biochem Biophys. 1955;59(2):491-501.
90. Fritz I. The effect of muscle extracts on the oxidation of palmitic acid by liver slices and homogenates. Acta Physiol Scand. 1955;34(4):367-85.
91. Bremer J. Carnitine in intermediary metabolism. The metabolism of fatty acid esters of carnitine by mitochondria. J Biol Chem. 1962;237:3628-32.
92. Hoppel CL, Tomec RJ. Carnitine palmityltransferase. Location of two enzymatic activities in rat liver mitochondria. J Biol Chem. 1972;247(3):832-41.
93. Pande SV. A mitochondrial carnitine acylcarnitine translocase system. Proc Natl Acad Sci U S A. 1975;72(3):883-7.
94. Mingrone G, Greco AV, Capristo E, Benedetti G, Giancaterini A, De Gaetano A, Gasbarrini G. L-carnitine improves glucose disposal in type 2 diabetic patients. J Am Coll Nutr. 1999;18(1):77-82.
95. Stephens FB, Constantin-Teodosiu D, Laithwaite D, Simpson EJ, Greenhaff PL. An acute increase in skeletal muscle carnitine content alters fuel metabolism in resting human skeletal muscle. J Clin Endocrinol Metab. 2006;91(12):5013-8.
96. Garrett Q, Xu S, Simmons PA, Vehige J, Flanagan JL, Willcox MD. Expression and localization of carnitine/organic cation transporter OCTN1 and OCTN2 in ocular epithelium. Invest OphthalmolVisSci. 2008;49(11):4844-9.
97. Pescosolido N, Imperatrice B, Koverech A, Messano M. L-carnitine and short chain ester in tears from patients with dry eye. Optom Vis Sci. 2009;86(2):E132-8.
98. Corrales RM, Luo L, Chang EY, Pflugfelder SC. Effects of osmoprotectants on hyperosmolar stress in cultured human corneal epithelial cells. Cornea. 2008;27(5):574-9.
99. Garrett Q SS, Simmons PA, Vehige Jr. JG, Willcox M. Carnitine and the Potential Osmoprotectants Protect Corneal Epithelial Cells from Hyperosmolar Solution Induced Damage. Investigative Ophthalmology & Visual Science 2010;51:2362.
100. Khandekar N, Willcox MD, Shih S, Simmons P, Vehige J, Garrett Q. Decrease in hyperosmotic stress-induced corneal epithelial cell apoptosis by L-carnitine. Mol Vis. 2013;19:1945-56.
101. Guillon M, Maissa C, Ho S. Evaluation of the effects on conjunctival tissues of Optive eyedrops over one month usage. Cont Lens Anterior Eye. 2010;33(2):93-9.
102. Shamsi FA, Chaudhry IA, Boulton ME, Al-Rajhi AA. L-carnitine protects human retinal pigment epithelial cells from oxidative damage. CurrEye Res. 2007;32(6):575-84.
103. Turan E, Valtink M, Reinach PS, Skupin A, Luo H, Brockmann T, Ba Salem MHO, Pleyer U, Mergler S. L-carnitine suppresses transient receptor potential vanilloid type 1 activity and myofibroblast transdifferentiation in human corneal keratocytes. Lab Invest. 2021;101(6):680-9.
104. Zorn-Kruppa M, Tykhonova S, Belge G, Bednarz J, Diehl HA, Engelke M. A human corneal equivalent constructed from SV40-immortalised corneal cell lines. Altern Lab Anim. 2005;33(1):37-45.
105. Manzer AK, Lombardi-Borgia S, Schafer-Korting M, Seeber J, Zorn-Kruppa M, Engelke M. SV40-transformed human corneal keratocytes: optimisation of serum-free culture conditions. ALTEX. 2009;26(1):33-9.
106. Grynkiewicz G, Poenie M, Tsien RY. A new generation of Ca2+ indicators with greatly improved fluorescence properties. J Biol Chem. 1985;260(6):3440-50.
107. Clapham DE. Calcium signaling. Cell. 2007;131(6):1047-58.
108. Capiod T. Extracellular Calcium Has Multiple Targets to Control Cell Proliferation. Adv Exp Med Biol. 2016;898:133-56.
109. Toth AB, Shum AK, Prakriya M. Regulation of neurogenesis by calcium signaling. Cell Calcium. 2016;59(2-3):124-34.
110. La Rovere RM, Roest G, Bultynck G, Parys JB. Intracellular Ca(2+) signaling and Ca(2+) microdomains in the control of cell survival, apoptosis and autophagy. Cell Calcium. 2016;60(2):74-87.

111. Turker E, Garreis F, Khajavi N, Reinach PS, Joshi P, Brockmann T, Lucius A, Ljubojevic N, Turan E, Cooper D, Schick F, Reinholz R, Pleyer U, Kohrle J, Mergler S. Vascular Endothelial Growth Factor (VEGF) Induced Downstream Responses to Transient Receptor Potential Vanilloid 1 (TRPV1) and 3-Iodothyronamine (3-T1AM) in Human Corneal Keratocytes. Front Endocrinol (Lausanne). 2018;9:670.
112. Voets T, Droogmans G, Wissenbach U, Janssens A, Flockerzi V, Nilius B. The principle of temperature-dependent gating in cold- and heat-sensitive TRP channels. Nature. 2004;430(7001):748-54.
113. Bruggemann A, Stoelzle S, George M, Behrends JC, Fertig N. Microchip technology for automated and parallel patch-clamp recording. Small. 2006;2(7):840-6.
114. Fertig N, Blick RH, Behrends JC. Whole cell patch clamp recording performed on a planar glass chip. Biophysical Journal. 2002;82(6):3056-62.
115. Barry PH. JPCalc, a software package for calculating liquid junction potential corrections in patch-clamp, intracellular, epithelial and bilayer measurements and for correcting junction potential measurements. J Neurosci Methods. 1994;51(1):107-16.
116. Bereiter DA, Rahman M, Thompson R, Stephenson P, Saito H. TRPV1 and TRPM8 Channels and Nocifensive Behavior in a Rat Model for Dry Eye. Invest Ophthalmol Vis Sci. 2018;59(8):3739-46.
117. Yang Y, Yang H, Wang Z, Varadaraj K, Kumari SS, Mergler S, Okada Y, Saika S, Kingsley PJ, Marnett LJ, Reinach PS. Cannabinoid receptor 1 suppresses transient receptor potential vanilloid 1-induced inflammatory responses to corneal injury. Cell Signal. 2013;25(2):501-11.
118. Gao Y, Zhang Y, Ru YS, Wang XW, Yang JZ, Li CH, Wang HX, Li XR, Li B. Ocular surface changes in type II diabetic patients with proliferative diabetic retinopathy. Int J Ophthalmol. 2015;8(2):358-64.
119. Alamri A, Bron R, Brock JA, Ivanusic JJ. Transient receptor potential cation channel subfamily V member 1 expressing corneal sensory neurons can be subdivided into at least three subpopulations. Front Neuroanat. 2015;9:71.
120. Garreis F, Schroder A, Reinach PS, Zoll S, Khajavi N, Dhandapani P, Lucius A, Pleyer U, Paulsen F, Mergler S. Upregulation of Transient Receptor Potential Vanilloid Type-1 Channel Activity and Ca2+ Influx Dysfunction in Human Pterygial Cells. Invest Ophthalmol Vis Sci. 2016;57(6):2564-77.
121. Yang H, Wang Z, Capo-Aponte JE, Zhang F, Pan Z, Reinach PS. Epidermal growth factor receptor transactivation by the cannabinoid receptor (CB1) and transient receptor potential vanilloid 1 (TRPV1) induces differential responses in corneal epithelial cells. Exp Eye Res. 2010;91(3):462-71.
122. Vriens J, Appendino G, Nilius B. Pharmacology of vanilloid transient receptor potential cation channels. Mol Pharmacol. 2009;75(6):1262-79.
123. Yang Y, Yang H, Wang Z, Mergler S, Wolosin JM, Reinach PS. Functional TRPV1 expression in human corneal fibroblasts. Exp Eye Res. 2013;107:121-9.
124. Lucius A, Khajavi N, Reinach PS, Kohrle J, Dhandapani P, Huimann P, Ljubojevic N, Grotzinger C, Mergler S. 3-Iodothyronamine increases transient receptor potential melastatin channel 8 (TRPM8) activity in immortalized human corneal epithelial cells. Cell Signal. 2016;28(3):136-47.
125. Zaelzer C, Hua P, Prager-Khoutorsky M, Ciura S, Voisin DL, Liedtke W, Bourque CW. DeltaN-TRPV1: A Molecular Co-detector of Body Temperature and Osmotic Stress. Cell Rep. 2015;13(1):23-30.
126. Bennett DJ, Kirby GW. Constitution and biosynthesis of capsaicin. J Chem Soc (C). 1968:442.
127. Hanson SM, Newstead S, Swartz KJ, Sansom MSP. Capsaicin interaction with TRPV1 channels in a lipid bilayer: molecular dynamics simulation. Biophys J. 2015;108(6):1425-34.
128. Chapa-Oliver AM, Mejia-Teniente L. Capsaicin: From Plants to a Cancer-Suppressing Agent. Molecules. 2016;21(8).
129. Baudouin C, Cochener B, Pisella PJ, Girard B, Pouliquen P, Cooper H, Creuzot-Garcher C. Randomized, phase III study comparing osmoprotective carboxymethylcellulose with sodium hyaluronate in dry eye disease. Eur J Ophthalmol. 2012;22(5):751-61.
130. Evangelista M, Koverech A, Messano M, Pescosolido N. Comparison of three lubricant eye drop solutions in dry eye patients. Optom Vis Sci. 2011;88(12):1439-44.
131. Hazarbassanov RM, Queiroz-Hazarbassanov NGT, Barros JN, Gomes JAP. Topical Osmoprotectant for the Management of Postrefractive Surgery-Induced Dry Eye Symptoms: A Randomised Controlled Double-Blind Trial. J Ophthalmol. 2018;2018:4324590.

132. Nebbioso M, Evangelista M, Librando A, Plateroti AM, Pescosolido N. Iatrogenic dry eye disease: an eledoisin/carnitine and osmolyte drops study. Biomed Pharmacother. 2013;67(7):659-63.
133. Hua X, Deng R, Li J, Chi W, Su Z, Lin J, Pflugfelder SC, Li DQ. Protective Effects of L-Carnitine Against Oxidative Injury by Hyperosmolarity in Human Corneal Epithelial Cells. Invest Ophthalmol Vis Sci. 2015;56(9):5503-11.
134. Hua X, Su Z, Deng R, Lin J, Li DQ, Pflugfelder SC. Effects of L-carnitine, erythritol and betaine on pro-inflammatory markers in primary human corneal epithelial cells exposed to hyperosmotic stress. Curr Eye Res. 2015;40(7):657-67.
135. Messmer EM. [Osmoprotection as a new therapeutic principle]. Ophthalmologe. 2007;104(11):987-90.
136. Deng R, Su Z, Hua X, Zhang Z, Li DQ, Pflugfelder SC. Osmoprotectants suppress the production and activity of matrix metalloproteinases induced by hyperosmolarity in primary human corneal epithelial cells. Mol Vis. 2014;20:1243-52.
137. Schrage NF, Flick S, von FT, Reim M, Wenzel M. [Temperature changes of the cornea by applying an eye bandage]. Ophthalmologe. 1997;94(7):492-5.
138. Xu S, Flanagan JL, Simmons PA, Vehige J, Willcox MD, Garrett Q. Transport of L-carnitine in human corneal and conjunctival epithelial cells. Molecular Vision. 2010;16:1823-31.
139. Mergler S, Derckx R, Reinach PS, Garreis F, Bohm A, Schmelzer L, Skosyrski S, Ramesh N, Abdelmessih S, Polat OK, Khajavi N, Riechardt AI. Calcium regulation by temperature-sensitive transient receptor potential channels in human uveal melanoma cells. Cell Signal. 2014;26(1):56-69.
140. Wang L, Dai W, Lu L. Hyperosmotic stress-induced corneal epithelial cell death through activation of Polo-like kinase 3 and c-Jun. Invest Ophthalmol Vis Sci. 2011;52(6):3200-6.
141. Yeh S, Song XJ, Farley W, Li DQ, Stern ME, Pflugfelder SC. Apoptosis of ocular surface cells in experimentally induced dry eye. Investigative Ophthalmology & Visual Science. 2003;44(1):124-9.
142. Luo L, Li DQ, Doshi A, Farley W, Corrales RM, Pflugfelder SC. Experimental dry eye stimulates production of inflammatory cytokines and MMP-9 and activates MAPK signaling pathways on the ocular surface. Invest Ophthalmol Vis Sci. 2004;45(12):4293-301.
143. Corrales RM, Stern ME, De Paiva CS, Welch J, Li DQ, Pflugfelder SC. Desiccating stress stimulates expression of matrix metalloproteinases by the corneal epithelium. Invest Ophthalmol Vis Sci. 2006;47(8):3293-302.
144. Jones DT, Monroy D, Ji Z, Pflugfelder SC. Alterations of ocular surface gene expression in Sjogren's syndrome. Adv Exp Med Biol. 1998;438:533-6.
145. Pflugfelder SC, Jones D, Ji Z, Afonso A, Monroy D. Altered cytokine balance in the tear fluid and conjunctiva of patients with Sjogren's syndrome keratoconjunctivitis sicca. Curr Eye Res. 1999;19(3):201-11.
146. Sobrin L, Liu Z, Monroy DC, Solomon A, Selzer MG, Lokeshwar BL, Pflugfelder SC. Regulation of MMP-9 activity in human tear fluid and corneal epithelial culture supernatant. Invest Ophthalmol Vis Sci. 2000;41(7):1703-9.
147. Pflugfelder SC, Solomon A, Stern ME. The diagnosis and management of dry eye: a twenty-five-year review. Cornea. 2000;19(5):644-9.
148. Fini ME, Cook JR, Mohan R. Proteolytic mechanisms in corneal ulceration and repair. Arch Dermatol Res. 1998;290 Suppl:S12-23.
149. Li DQ, Meller D, Liu Y, Tseng SC. Overexpression of MMP-1 and MMP-3 by cultured conjunctivochalasis fibroblasts. Invest Ophthalmol Vis Sci. 2000;41(2):404-10.
150. Li DQ, Lee SB, Gunja-Smith Z, Liu Y, Solomon A, Meller D, Tseng SC. Overexpression of collagenase (MMP-1) and stromelysin (MMP-3) by pterygium head fibroblasts. Arch Ophthalmol. 2001;119(1):71-80.
151. Dursun D, Kim MC, Solomon A, Pflugfelder SC. Treatment of recalcitrant recurrent corneal erosions with inhibitors of matrix metalloproteinase-9, doxycycline and corticosteroids. Am J Ophthalmol. 2001;132(1):8-13.

152. Traina G, Bernardi R, Cataldo E, Macchi M, Durante M, Brunelli M. In the rat brain acetyl-L-carnitine treatment modulates the expression of genes involved in neuronal ceroid lipofuscinosis. Mol Neurobiol. 2008;38(2):146-52.
153. Origlia N, Migliori M, Panichi V, Filippi C, Bertelli A, Carpi A, Giovannini L. Protective effect of L-propionylcarnitine in chronic cyclosporine-a induced nephrotoxicity. Biomed Pharmacother. 2006;60(2):77-81.
154. Iliceto S, Scrutinio D, Bruzzi P, D'Ambrosio G, Boni L, Di Biase M, Biasco G, Hugenholtz PG, Rizzon P. Effects of L-carnitine administration on left ventricular remodeling after acute anterior myocardial infarction: the L-Carnitine Ecocardiografia Digitalizzata Infarto Miocardico (CEDIM) Trial. J Am Coll Cardiol. 1995;26(2):380-7.
155. Ferrari R, Merli E, Cicchitelli G, Mele D, Fucili A, Ceconi C. Therapeutic effects of L-carnitine and propionyl-L-carnitine on cardiovascular diseases: a review. Ann N Y Acad Sci. 2004;1033:79-91.
156. Sima AA. Acetyl-L-carnitine in diabetic polyneuropathy: experimental and clinical data. CNS Drugs. 2007;21 Suppl 1:13-23; discussion 45-6.
157. Therrien G, Rose C, Butterworth J, Butterworth RF. Protective effect of L-carnitine in ammonia-precipitated encephalopathy in the portacaval shunted rat. Hepatology. 1997;25(3):551-6.
158. Pessotto P, Liberati R, Petrella O, Romanelli L, Calvani M, Peluso G. In experimental diabetes the decrease in the eye of lens carnitine levels is an early important and selective event. Exp Eye Res. 1997;64(2):195-201.
159. Roomets E, Kivela T, Tyni T. Carnitine palmitoyltransferase I and Acyl-CoA dehydrogenase 9 in retina: insights of retinopathy in mitochondrial trifunctional protein defects. Invest Ophthalmol Vis Sci. 2008;49(4):1660-4.
160. Dworkin RH, Johnson RW, Breuer J, Gnann JW, Levin MJ, Backonja M, Betts RF, Gershon AA, Haanpaa ML, McKendrick MW, Nurmikko TJ, Oaklander AL, Oxman MN, Pavan-Langston D, Petersen KL, Rowbotham MC, Schmader KE, Stacey BR, Tyring SK, van Wijck AJ, Wallace MS, Wassilew SW, Whitley RJ. Recommendations for the management of herpes zoster. Clin Infect Dis. 2007;44 Suppl 1:S1-26.
161. Bhatti MT, Patel R. Neuro-ophthalmic considerations in trigeminal neuralgia and its surgical treatment. Curr Opin Ophthalmol. 2005;16(6):334-40.
162. Lambiase A, Manni L, Bonini S, Rama P, Micera A, Aloe L. Nerve growth factor promotes corneal healing: structural, biochemical, and molecular analyses of rat and human corneas. Invest Ophthalmol Vis Sci. 2000;41(5):1063-9.
163. You L, Kruse FE, Volcker HE. Neurotrophic factors in the human cornea. Invest Ophthalmol Vis Sci. 2000;41(3):692-702.
164. Di G, Qi X, Zhao X, Zhang S, Danielson P, Zhou Q. Corneal Epithelium-Derived Neurotrophic Factors Promote Nerve Regeneration. Invest Ophthalmol Vis Sci. 2017;58(11):4695-702.
165. Micera A, Lambiase A, Puxeddu I, Aloe L, Stampachiacchiere B, Levi-Schaffer F, Bonini S, Bonini S. Nerve growth factor effect on human primary fibroblastic-keratocytes: possible mechanism during corneal healing. Exp Eye Res. 2006;83(4):747-57.
166. Okada Y, Reinach PS, Shirai K, Kitano A, Kao WW, Flanders KC, Miyajima M, Liu H, Zhang J, Saika S. TRPV1 involvement in inflammatory tissue fibrosis in mice. Am J Pathol. 2011;178(6):2654-64.
167. Yang Y, Yang H, Wang Z, Okada Y, Saika S, Reinach PS. Wakayama symposium: dependence of corneal epithelial homeostasis on transient receptor potential function. Ocul Surf. 2013;11(1):8-11.
168. Saika S, Yamanaka O, Okada Y, Sumioka T. Modulation of Smad signaling by non-TGFbeta components in myofibroblast generation during wound healing in corneal stroma. Exp Eye Res. 2016;142:40-8.
169. Khajavi N, Reinach PS, Slavi N, Skrzypski M, Lucius A, Strauss O, Kohrle J, Mergler S. Thyronamine induces TRPM8 channel activation in human conjunctival epithelial cells. Cell Signal. 2015;27(2):315-25.
170. Khajavi N, Mergler S, Biebermann H. 3-Iodothyronamine, a Novel Endogenous Modulator of Transient Receptor Potential Melastatin 8? Front Endocrinol (Lausanne). 2017;8:198.

171. Chen GL, Lei M, Zhou LP, Zeng B, Zou F. Borneol Is a TRPM8 Agonist that Increases Ocular Surface Wetness. PLoS One. 2016;11(7):e0158868.
172. Wu CJ, Huang QW, Qi HY, Guo P, Hou SX. Promoting effect of borneol on the permeability of puerarin eye drops and timolol maleate eye drops through the cornea in vitro. Pharmazie. 2006;61(9):783-8.
173. Bajpai R, Lesperance J, Kim M, Terskikh AV. Efficient propagation of single cells Accutase-dissociated human embryonic stem cells. MolReprodDev. 2008;75(5):818-27.
174. Hamill OP, Marty A, Neher E, Sakmann B, Sigworth FJ. Improved patch-clamp techniques for high-resolution current recording from cells and cell-free membrane patches. Pflugers Arch. 1981;391(2):85-100.

Statutory Declaration

“I, Elizabeth Turan, by personally signing this document in lieu of an oath, hereby affirm that I prepared the submitted dissertation on the topic “Influence of L-carnitine on transient receptor potential vanilloid 1 (TRPV1) activity in human corneal keratocytes“ independently and without the support of third parties, and that I used no other sources and aids than those stated.
All parts which are based on the publications or presentations of other authors, either in letter or in spirit, are specified as such in accordance with the citing guidelines. The sections on methodology (in particular regarding practical work, laboratory regulations, statistical processing) and results (in particular regarding figures, charts and tables) are exclusively my responsibility.

Furthermore, I declare that I have correctly marked all of the data, the analyses, and the conclusions generated from data obtained in collaboration with other persons, and that I have correctly marked my own contribution and the contributions of other persons (cf. declaration of contribution). I have correctly marked all texts or parts of texts that were generated in collaboration with other persons.

My contributions to any publications to this dissertation correspond to those stated in the below joint declaration made together with the supervisor. All publications created within the scope of the dissertation comply with the guidelines of the ICMJE (International Committee of Medical Journal Editors; www.icmje.org) on authorship. In addition, I declare that I shall comply with the regulations of Charité – Universitätsmedizin Berlin on ensuring good scientific practice.

I declare that I have not yet submitted this dissertation in identical or similar form to another Faculty.

The significance of this statutory declaration and the consequences of a false statutory declaration under criminal law (Sections 156, 161 of the German Criminal Code) are known to me.”

Date Signature

Declaration of my own contribution to any publications

Elizabeth Turan contributed the following to the below listed publications:

Publication 1: Turker E, Garreis F, Khajavi N, Reinach PS, Joshi P, Brockmann T, Lucius A, Ljubojevic N, Turan E, Cooper D, Schick F, Reinholz R, Pleyer U, Kohrle J, Mergler S. Vascular endothelial growth factor (VEGF) induced downstream responses to transient receptor potential vanilloid 1 (TRPV1) and 3-Iodothyronamine (3-T1AM) in human corneal keratocytes. Front Endocrinol (Lausanne). 2018;9:670.

Contribution: Calcium imaging and planar patch-clamp experiments with SV40-transfected HCK cells and the use of CAP as well as L-carnitine were performed by Elizabeth Turan. Figure 5 (A-F) was created on the basics of Elizabeth Turans statistical evaluation under the supervision of Dr. Stefan Mergler.

Publication 2: Turan E, Valtink M, Reinach PS, Skupin A, Luo H, Brockmann T, Ba Salem MHO, Pleyer U, Mergler S. L-carnitine suppresses transient receptor potential vanilloid type 1 activity and myofibroblast transdifferentiation in human corneal keratocytes. Lab Invest. 2021;101(6):680-9.

Contribution: Elizabeth Turan and Stefan Mergler designed the study, wrote and edited the manuscript. Elizabeth Turan performed calcium imaging measurements and planar patch-clamp recordings with SV40-transfected HCK cells. Figures 2 (A-E), 3 (A-C), 4 (A-C), and 5 (A-C) were created by Elizabeth Turan on the basics of her statistical evaluation under the supervision of Dr. Stefan Mergler.

_____

Signature, date and stamp of first supervising university professor / lecturer

_____

Signature of doctoral candidate

Curriculum Vitae

Due to privacy settings, the Curriculum Vitae will not be displayed in the online version of this document.

List of publications

1. Turker E, Garreis F, Khajavi N, Reinach PS, Joshi P, Brockmann T, Lucius A, Ljubojevic N, Turan E, Cooper D, Schick F, Reinholz R, Pleyer U, Kohrle J, Mergler S. Vascular endothelial growth factor (VEGF) induced downstream responses to transient receptor potential vanilloid 1 (TRPV1) and 3-Iodothyronamine (3-T1AM) in human corneal keratocytes. Front Endocrinol (Lausanne). 2018;9:670.
2. Turan E, Valtink M, Reinach PS, Skupin A, Luo H, Brockmann T, Ba Salem MHO, Pleyer U, Mergler S. L-carnitine suppresses transient receptor potential vanilloid type 1 activity and myofibroblast transdifferentiation in human corneal keratocytes. Lab Invest. 2021;101(6):680-9.

Acknowledgements

All experimental data contained in this thesis were generated at the research Department of Ophthalmology (Experimental Ophthalmology) at the Campus Virchow Clinic, Charité University of Medicine, Berlin. At this point, I would like to thank every person who has accompanied me during this instructive journey and helped me finishing my thesis:

Firstly, I want to thank my supervisor PD Dr. phil. nat. Stefan Mergler (Department of Ophthalmology, Charité – University of Medicine, Berlin) for assigning this topic to me and introducing me to scientific work. Without his generous support during the whole process, this work would have been impossible. I am sincerely grateful for the opportunity to learn from him and work with him on these challenging projects.

I would also like to thank my second supervisor Prof. Dr. med. Uwe Pleyer (Department of Ophthalmology, Charité – University of Medicine, Berlin) for the helpful discussions and support during the experimental and publication process. It was a great honor for me to work with him.

I also appreciate the support of PhD Dr. Peter S. Reinach (School of Ophthalmology and Optometry, Wenzhou Medical University, China) for his competent expertise in TRP channel research and great help regarding our manuscript and this thesis. Special thanks to Dr. rer. nat. Michaela Zorn-Kruppa (University Medical Center Hamburg-Eppendorf) for providing us the SV40-transfected HCK cells.

Last but not least, I want to thank my parents Neil and Sariye Turan. Throughout my entire life, they have always motivated me in everything I do. Without their unlimited support, I would not be the person I am today. Therefore, I am deeply thankful and beyond blessed. This doctoral thesis is for you. I love you!